Hydrological downscaling of soil moisture

Günter Blöschl[1], Jürgen Komma[1], Stefan Hasenauer[2]

[1] Institute of Hydraulic Engineering and Water Resources Management
[2] Institute of Photogrammetry and Remote Sensing
Vienna University of Technology
A-1040 Vienna, Austria

Final Report to the H-SAF (Hydrology Satellite Application Facility) via the Austrian Central Institute for Meteorology and Geodynamics (ZAMG)

"Visiting scientists programme"
December 2009

1. Introduction

Soil moisture has an important influence on hydrological and meteorological processes. Soil moisture is the main control of processes that partition rainfall into runoff and infiltration. Extreme hydrological events (floods and droughts) often have a large socio-economical impact and are strongly modulated by the soil moisture state of the landscape. Accurate estimates of soil moisture are hence important for a range of hydrological applications including flood and drought forecasting systems as well as hydrological assessment models. A realistic representation of the spatial variability of near surface soil moisture is also critically important for representing hydrological fluxes in the subsurface at various scales (Zehe and Blöschl, 2004) and for linking hydrological processes with atmospheric processes (Ronda et al. 2002; Montaldo and Albertson, 2003).

Wagner et al. (2003) developed a soil moisture retrieval method for space-borne scatterometer systems that has been shown to produce accurate results in a number of settings (e.g. Scipal, 2002). The satellite based monitoring is particularly appealing for large regions as it tends to cover large areas, and in an operational context, because of the regular sampling frequency. It is clear that the scatterometer data contain a lot of useful information on the spatial and temporal soil moisture dynamics. Methods of refined soil moisture retrieval are currently being developed by the Institute of Remote Sensing and Photogrammetry of the Vienna University of Technology as part of an H-SAF project. In the H-SAF project, the focus is on a relatively coarse spatial resolution as consistent with the sensor characteristics. However, there is significant spatial variation in soil moisture at a much finer scale and much of this small scale variability controls the runoff response from catchments. In turn, this small scale soil moisture variability is controlled by topography, soil type, precipitation and vegetation (Western et al., 2002), among other factors. This small scale variability cannot be resolved by the scatterometer data. Most hydrological applications that are of practical relevance cover catchment scales of a few to thousands of square kilometres and one is interested in the spatial distribution of soil moisture *within* these catchments. In contrast, the pixel resolution of the scatterometer data is on the order of ten thousand square kilometres, so is unable to resolve the within catchment variability of soil moisture. It would hence be extremely useful to downscale the scatterometer data to finer space scales based on hydrological concepts. This is the topic of the project reported here.

There are two basic issues of soil moisture upscaling/downscaling in the hydrological sciences. The first is how to best estimate average catchment soil moisture (or spatial distributions) from point soil moisture measured in the field, the second is how to best estimate patterns of soil moisture from catchment average soil moisture as measured by satellite sensors. The first issue is an upscaling task while the second one is downscaling. In both instances one can use deterministic process based models which is dealt with in Grayson and Blöschl (2000a) and Pitman (2003). Alternatively one can use simplified statistical descriptions that aim at representing the most important controls and these will be briefly reviewed here. These methods can either exploit the spatial statistics of soil moisture or make use of auxiliary information in terms of a moisture index (Blöschl, 2005; Western et al., 2002, 2003).

(a) Methods based on the spatial statistics: A number of authors have suggested that the spatial distribution function of soil moisture can be approximated by a normal distribution although the shape of the distribution does change with climate (e.g. Mohanty et al., 2000; Nyberg, 1996). The variance of the spatial distribution of soil moisture, when taking numerous studies around the world together (Western et al., 2003) tends to depend on mean catchment moisture, indicating a pattern of variance that increases from near zero at wilting point to a peak at moderate moisture levels and then decreases to near zero as the mean moisture approaches saturation. Understanding of the spatial distribution of soil moisture has been used in distribution models to estimate runoff generation and evaporation (Beven, 1995; Wood et al., 1992; Zhao, 1992). It is interesting that the shape of the distribution functions varies widely between models but the models are similarly successful in predicting catchment runoff.

Studies on the spatial correlation of soil moisture have been summarised by Western et al. (2004). Typical correlation lengths vary between 1 m and 600 m and there is a tendency for the correlation lengths to increase with extent and spacing of the data as would be expected given the sampling scale effects (see, e.g., Skøien and Blöschl, 2006ab). While some of the small scale catchment studies suggest that the spatial soil moisture variability is stationary, analyses of remotely sensed soil moisture have found fractal behaviour (e.g. Hu et al., 1997). Ground based point data collected over large areas in the Former Soviet Union, Mongolia, China and the USA suggest that soil moisture variation could be represented as a stationary field with a correlation length of about 400 – 800 km (Entin et al., 2000). Part of the differences in correlation lengths in small scale and large scale studies may, again, be related

to sampling effects, although there also appear to exist important changes in the process controls with scale causing such differences. Over short scales, climate may be relatively uniform and the variation may be mainly related to differences in soils and vegetation (Seyfried, 1998) while at larger scales climate may be a dominant source of soil moisture variability. Methods of upscaling and downscaling that are based on the spatial statistics involve a wide spectrum of geostatistical methods to obtain spatial patterns or averages from point data or to obtain spatial patterns from catchment average soil moisture (e.g. Deutsch and Journel, 1992). These methods include conditional simulation methods based on the assumption that soil moisture is a Gaussian random field. Geostatistical methods can also be used to derive analytical estimates of how, say, the runoff contributing area in a distributed model will change with grid size (Western and Blöschl, 1999).

(b) Index approach: In the index approach spatial organisation can be imposed on the soil moisture field that goes beyond the Gaussian random field of the previous method by using landscape characteristics. These characteristics are usually condensed into an index for numerical efficiency guided by the understanding one has about the movement of water in the landscape (Moore et al., 1991). In humid climates, lateral redistribution of moisture by shallow subsurface flow can be an important process and in this case, indices reflecting upslope area, slope, or convergence should be related to the soil moisture. The most commonly used index is the topographic wetness index of Beven and Kirkby (1979) (see also O'Loughlin, 1986) which is a function of the specific contributing area (being an index of the precipitation forcing) and the surface slope (being an index of the resistance of the soil to lateral flows). Terrain data are widely available and there exists sophisticated terrain analysis software (Wilson and Gallant 2000). Because of this, the wetness index is widely used for upscaling and downscaling soil moisture. The index involves a number of assumptions some of which have been relaxed. Barling et al. (1994), for example, relaxed the steady-state assumption and Woods et al. (1997) relaxed the assumption of uniform recharge. Western et al. (1999, 2002) examined the predictive ability of various terrain indices against soil moisture data collected in a small humid catchment in south-east Australia. The wetness index typically explained 50% of the spatial soil moisture variance during the wet season (Figure 1a) and there were other indices that showed a similar performance such as the tangent curvature of the terrain (Figure 1b). The largest soil moisture values were collected in the gullies that exhibit large specific contributing areas and strongly negative tangent curvature. However, as the catchment dried out, the explanatory power of the indices dropped off rapidly. Western et al. (1999) also summarised tests of terrain indices in various climates and

noted that their predictive ability varies substantially, depending on whether their main assumptions are satisfied.

All of these indices can be used to estimate a spatial pattern (or a spatial distribution) from average catchment soil moisture (i.e. downscaling) and to estimate a spatial pattern from point measurements. In the latter case, similar geostatistical methods can be used as discussed above but they are extended to accommodate the index as an auxiliary variable. Methods include external drift kriging, co-kriging and georegression (e.g. Blöschl and Grayson, 2000). Examples of applications include Viney and Sivapalan (2004) who disaggregated areal average soil moisture into spatial patterns and Green and Erskine (2004) who compared a geostatistical analysis with linear geo-regression using terrain indices. In spite of the considerable progress that has been made in the past decades on soil moisture upscaling and downscaling there is still significant uncertainty involved because of the large natural variability in soil moisture and its controls. If only a few point soil moisture measurements are available in a catchment the errors associated with upscaling them to catchment averages can be enormous (Grayson et al., 2002). An interesting extension of the index approach has therefore been proposed by Grayson and Western (1998). They suggested that concepts of time stability, applied to catchments with significant relief, can be used to identify certain parts of the landscape which consistently exhibit mean behaviour irrespective of the overall wetness. They denoted these areas as catchment average soil moisture monitoring (CASMM) sites. This approach promises to assist in the upscaling issue if point measurements of soil moisture can be located in these areas. For downscaling satellite soil moisture data, a *combination* of the index approach and the time stability assumption based on the spatial statistics seems to be a useful strategy. The idea of the index approaches is to represent the main hydrological processes in a simplified way and with a limited number of input data. In an operational context, this type of downscaling method is hence very appealing and has been pursued in this project. The main controls that were taken into account are topography, soils, and climate. All of them are represented in a simple and robust way.

The aim of the study was to develop a downscaling method for scatterometer soil moisture data that allows to infer spatial patterns of soil moisture at a scale of a few square kilometres from the original scale of ten thousand square kilometres, based on hydrological concepts. The model was applied to scatterometer soil moisture data for all of Europe to assess the plausibility of the method. As mentioned above, Western et al. (1999, 2002) indicated that the predictive performance of downscaling methods of soil moisture may be modest because of

the inherent uncertainty of soil hydrological processes. It is hence important to test the actual value of the method as compared to the alternative of using the original scatterometer data directly in hydrological applications. The downscaling method was hence tested against independent ENVISAT Advanced Synthetic Aperture Radar (ASAR) data. The purpose of the comparison is to assess the added value of the downscaling method over simply using the original (coarse resolution) scatterometer data in hydrological applications.

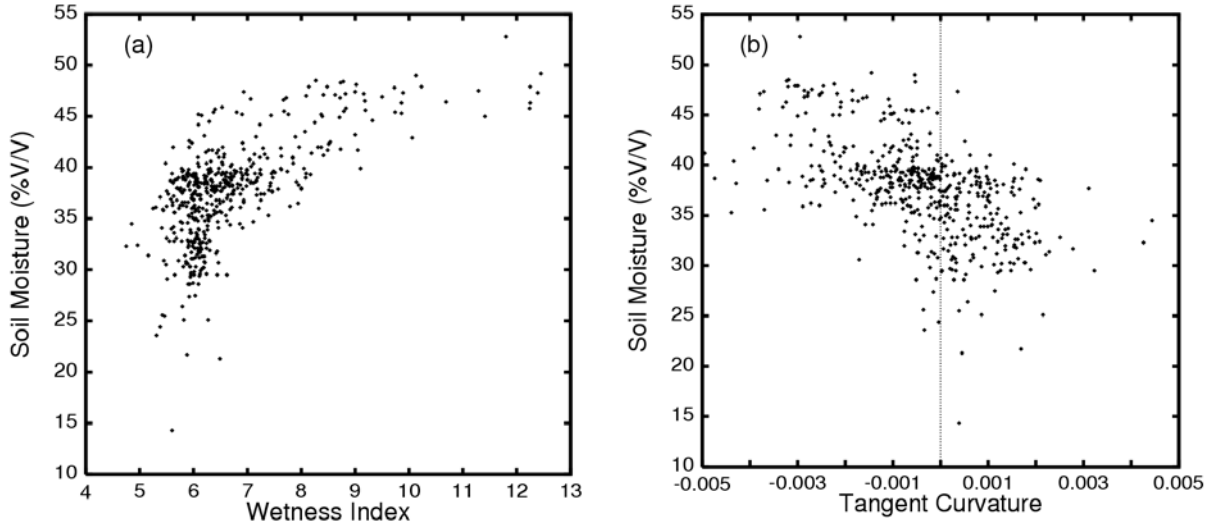

Figure 1: Relationship between volumetric soil moisture in the top 30 cm of the soil profile and wetness index, and tangent curvature for September 27, 1995 in the Tarrawarra catchment, Australia. From Western et al. (1999).

2. Downscaling model

The regional pixel scale in this study was chosen as 25 km which is an approximate pixel size of ERS scatterometer products of soil moisture. The local pixel scale was chosen as 1 km, which is consistent with hydrological modelling needs.

The downscaling model proposed here is

$$\Theta_L(\mathbf{x},t) = \xi(\mathbf{x}) \cdot b(\mathbf{x},t) + c(\mathbf{x},t) \qquad (1)$$

where Θ_L refers to the soil moisture at the local scale (1 km), ξ is the fingerprint which depends on space **x** but does not depend on time *t*. *b* and *c* are parameters that depend on both

time and space and are estimated as a function of the soil moisture Θ_R at the regional scale (25 km), i.e.

$$b = f(\Theta_R) \tag{2}$$

$$c = f(\Theta_R) \tag{3}$$

This downscaling model involves three assumptions:

- The small scale pattern of soil moisture does not change with time. This means that a static index pattern, the so called fingerprint, can be used to downscale soil moisture. The concepts of patterns not changing with time is discussed in more detail in Wagner et al. (2008). This assumption can be straightforwardly relaxed if more detailed information is available without violating the other assumptions of the model. The fingerprint has been obtained here from a conceptual hydrological model that represents the understanding of hydrological soil moisture processes at the grid scale. The processes include lateral flow in the soil related to saturation excess runoff generation; vertical flow in the soil related to infiltration excess runoff generation; and water logging or ponding when the groundwater table rises to the surface. The fingerprint is ξ in Eq. (1).

- The spatial variance of the soil moisture Θ_L at the local scale was estimated from the spatial variance of the soil moisture Θ_R at the regional scale using scaling theory. In essence, the main observation of the scaling theory is that the spatial variance decreases with the spatial aggregation scale (i.e. the support) and this property is exploited here. The spatial variance of the soil moisture at the local scale is related to the parameter *b* in Eq. (1).

- The spatial mean of the soil moisture Θ_L at the local scale was estimated from the spatial mean of the soil moisture Θ_R at the regional scale based on an unbiasedness constraint. This constraint is equivalent to the idea that soil moisture is mass conserving, so the regional scale soil moisture should be the spatial mean of the local soil moisture over a suitable aggregation area. The spatial mean of the soil moisture at the local scale is related to the parameter *c* in Eq. (1).

2.1 Fingerprints

The concept of fingerprints was gleaned from Steinacker et al. (2006) although the downscaling method proposed here differs from theirs. To obtain the fingerprints, a conceptual hydrological model of the spatial patterns of soil moisture was developed. The model recognises three types of runoff generation processes (Figure 2). The model follows the idea of the Dominant Processes Concept of Grayson and Blöschl (2000b) that focuses on a set of the most important processes in a particular context rather than on modelling the processes in their full complexity (see also Blöschl, 2001). Depending on the process type, the fingerprint is estimated from different data. The following three process types are considered:

Lateral flow in the soil and saturation excess runoff generation: This is the type of process often encountered in hilly terrain when runoff generation and soil moisture redistribution is dominated by lateral movement of soil moisture on the hillslopes. The fingerprint is modelled here as the balance of the forcing (rainfall) and the resistance (soils) similar to the wetness index of Beven and Kirkby (1979). Mean annual precipitation (*MAP*) was used for representing the forcing, terrain curvature (*curv*) was used for representing the resistance. The fingerprint is then calculated as the weighted mean of the two. The combination of *MAP* and *curv* implies large soil moisture in high rainfall areas and large soil moisture in valleys were the curvature is positive. Both *MAP* and *curv* were rescaled to unit standard deviations and combined to obtain the weighted mean:

$$\xi_1 = a \cdot MAP + (1-a) \cdot curv \tag{4}$$

where a was chosen in a way that the *MAP* component controls the pattern of ξ_1 in 60% of the study domain (i.e. Europe) while *curv* controls the pattern of ξ_1 in the remaining 40%. This type of process was considered to be dominant in hilly and steep terrain. A threshold of terrain slope >4° was chosen for this process to be applicable (Table 1). For terrain flatter than 0.1°, the processes discussed below were considered to be dominant (Figure 2).

Vertical flow in the soil and infiltration excess runoff generation: This type of process often occurs in flat terrain in two instances. The first is where the soils are deep, so water can freely infiltrate into the soil without the groundwater table rising to the surface. The main control in this case is the soil texture. The fingerprint was hence assumed to be related to soil texture:

$$\xi_{2a} = texture \tag{5}$$

where large grain sizes translate into a small value of the texture class and small grain sizes into a large value of the texture class. This means that sandy soils will produce relatively low soil moisture values while clays will produce large soil moisture values. The second instance is when the soils are shallow and the climate is relatively dry. In this case, again, the groundwater table will tend not to rise to the surface. Texture will again be the main control, so

$$\xi_{2b1} = texture \tag{6}$$

Soils were considered to be deep for soil depths >200 cm, and shallow for soil depths <20cm. The climate was assumed to be dry for mean annual precipitation MAP < 300mm/yr.

Water logging or ponding when the groundwater table rises to the surface: This type of process may occur in flat terrain when the climate is wet and preferably for shallow soils. If the groundwater table rises to the surface, one can assume that the soil moisture in the valleys and depressions will be higher than that on the hillslopes and tops. In valleys and depressions the curvature is positive while it is negative on the tops. The fingerprint was hence estimated from terrain curvature:

$$\xi_{2b1} = curv \tag{7}$$

A wet climate was assumed to exist with the mean annual precipitation was larger than 900 mm/yr.

All fingerprints were normalised to zero mean and unit standard deviation, where both the mean $\bar{\zeta}_i$ and the standard deviation σ_{ζ_i} were estimated from the fingerprints over the entire domain:

$$\zeta_i' = \frac{\zeta_i - \bar{\zeta}_i}{\sigma_{\zeta_i}} \tag{8}$$

The index *i* refers to the process type. The fingerprints for the three dominant process types were then combined based on the thresholds of Table 1. For the intermediate ranges, the combined fingerprint was estimated as a weighted mean, as indicted in Table 1. The combined fingerprint ξ' was again normalised to zero mean and unit standard deviation. However, in this case the mean $\bar{\zeta}'$ and the standard deviation $\sigma_{\zeta'}$ were estimated over the entire domain. The normalised combined fingerprint ξ has zero mean and unit standard deviation. ξ is a function of space but not a function of time.

Table 1: Thresholds used for the combined fingerprint ξ'.

Hydrologic characteristics	Lower threshold	Intermediate	Upper threshold
Mean annual precipitation MAP	<300 mm/yr	300-900 mm/yr	>900 mm/yr
ξ'_{2b} =	ξ'_{2b1}	weighted mean	ξ'_{2b2}
Soil depth	<20 mm	20-200 mm	>200 mm
ξ'_{2} =	ξ'_{2b}	weighted mean	ξ'_{2a}
Terrain slope	<0.1°	0.1-4°	>4°
ξ' =	ξ'_{2}	weighted mean	ξ'_{1}

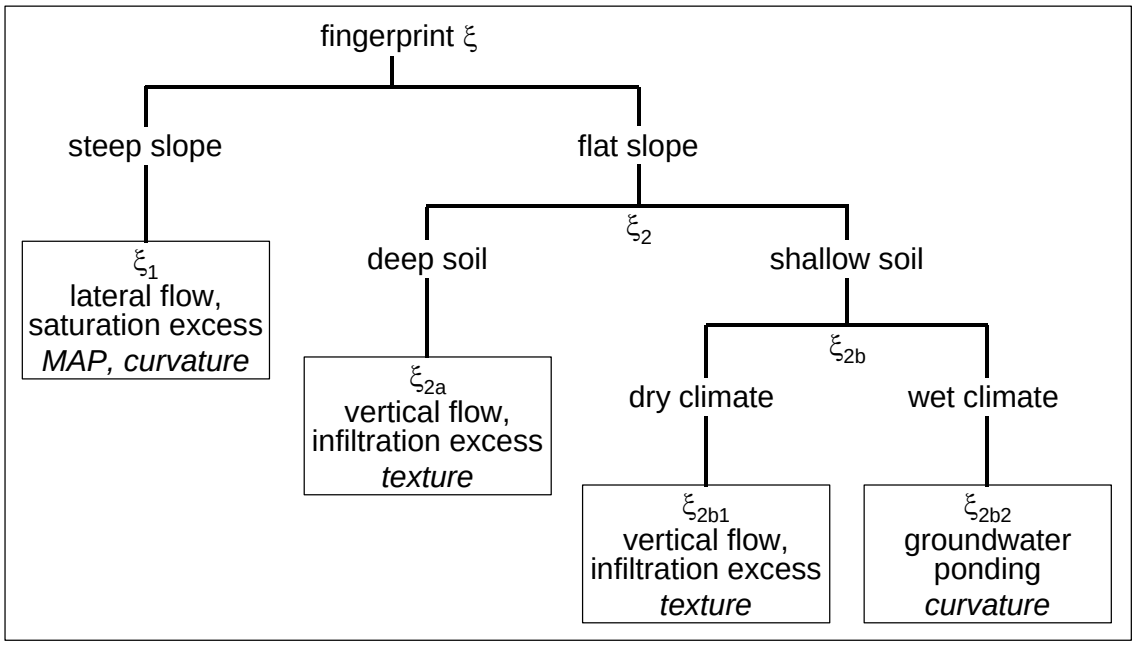

Figure 2: Conceptual hydrological model for the downscaling fingerprint.

2.2 Spatial variance

The spatial variance of the soil moisture Θ_L at the local scale was estimated from the spatial variance of the soil moisture Θ_R at the regional scale using scaling theory. Scaling theory relates the spatial variances at different support (or aggregation) scales. Because of the random elements in the spatial distribution of soil moisture, the spatial variance always decreases with support scale. The exact decrease is related to the spatial correlation structure of soil moisture. A number of studies have analyses the spatial correlation structure and the decrease of variance with support scale. Western et al. (1998, 2004) collected high-resolution soil moisture *in situ* data from the 10.5 ha Tarrawarra catchment in south-eastern Australia. For each survey, up to 1536 data points in space were used to analyse the spatial correlatin structure. Western and Blöschl (1999) analysed the scaling characteristics of these soil moisture data. They found the change in variance as shown in Figure 3. Based on an exponential model to represent the spatial correlations they were able to predict the decrease in variance with aggregation scale (solid line in Figure 3). Other studies reviewed in Western et al. (1998; 2002, p. 167; 2003, p. 135; 2004), Blöschl (1999), Merz et al. (2001) and Skøien et al. (2003) suggest however, that the spatial correlations are fractal (or close to fractal) if a wide range of scales is considered and measurement biases are small (also see the review in the introduction section of this report). A fractal correlation structure implies that the correlation is related to distance by a power law. A power law of the correlation translates into a power law in the decrease in variance. Power law scaling relationships are shown in Figure 3 with exponents of α = 0.25 and 0.35 respectively. These exponents are also consistent with the scaling behaviour of the topographic wetness index of Beven and Kirkby (1979) calculated for all of Austria (Figure 4).

Based on the literature evidence, the decrease in variance was assumed to follow a power law in this study:

$$\sigma_L^2 = \sigma_R^2 \cdot \left(\frac{L_L}{L_R}\right)^{-\alpha} \tag{9}$$

where σ_L^2 is the local variance (at the small grid scale), σ_R^2 is the regional variance (at the large grid scale), L_L and L_R are the grid sizes (length scales) of 1 km and 25 km, respectively, and α is the exponent of the scaling relationship. This scaling relationship was then applied in the following steps:

- Estimate the large scale variance σ_R^2 of soil moisture from subregions of 5x5 large-scale pixels.
- Interpolate this variance to the small scale grid using the centre of the large pixels as the reference points.
- Scale the variance to the small scale for each small scale pixel using Eq. (9) and an exponent of $\alpha = 0.35$.
- Multiply the fingerprint by the small scale standard deviation, i.e.,

$$\xi_L = \xi \cdot \sigma_L \tag{10}$$

- repeat the procedure for each small scale pixel.

$\xi_L(\mathbf{x},t)$ now represents the pattern of soil moisture at the small scale with the variance of the soil moisture but with zero mean, i.e., a biased soil moisture estimate.

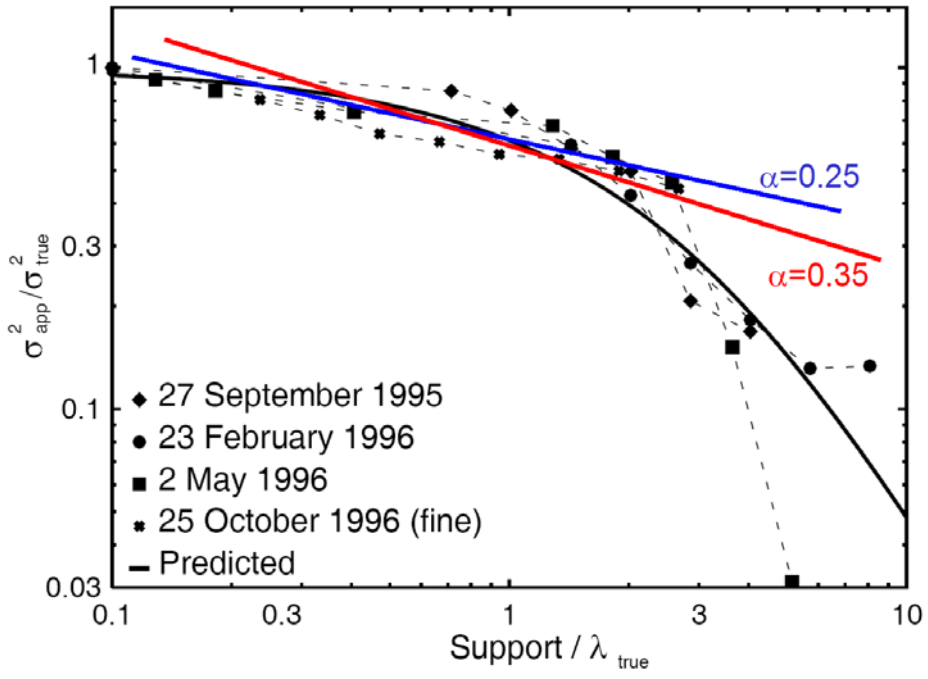

Figure 3: Variance reduction of *in situ* soil moisture data by aggregation. σ_{true}^2 is the variance of the *in situ* data, σ_{app}^2 is the apparent or aggregated variance, λ_{true} is the correlation length (m) of the *in situ* data, *Support* is the aggregation scale (m). The markers indicate data from four field surveys, the solid black line is the aggregation model of Western and Blöschl (1999), the blue and red lines relate to the power laws of Eq. (9). Figure from Western and Blöschl (1999, p. 214), modified.

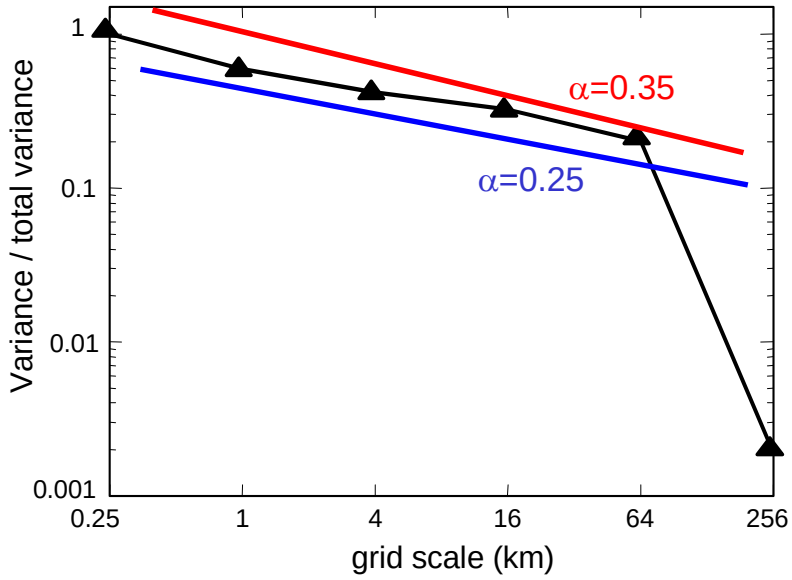

Figure 4: Variance reduction of the topographic wetness index of Beven and Kirkby (1979) calculated at a 250 m grid resolution for Austria. From Merz et al. (2001), modified.

2.3 Spatial mean

The spatial mean of the soil moisture Θ_L at the local scale was estimated from the spatial mean of the soil moisture Θ_R at the regional scale based on an unbiasedness constraint. This constraint is equivalent to the idea that soil moisture is mass conserving, so the regional scale soil moisture should be the spatial mean of the local soil moisture over a suitable aggregation area. The following steps were applied:

- Calculate the mean $\overline{\Theta}_R$ of the large scale soil moisture over a moving window with a size L_R, centred on each small scale pixel, by assuming that the soil moisture is spatially uniform within each large scale pixel.
- Calculate the mean $\overline{\xi}_L$ of the biased soil moisture estimate at the small scale over a moving window with a size L_R, centred on each small scale pixel.
- Account for the unbiasedness constraint:

$$\Theta_L = \xi_L + \overline{\Theta}_R - \overline{\xi}_L \tag{11}$$

Θ_L is then the downscaled soil moisture estimate. This final estimate was checked whether it exceeded a physically plausible range.

3. Data

In this study a range of earth-observation data (satellite data, soil data, model data) were used, which cover all of Europe. In time, the soil moisture data are from the period 2005-2007. The data are listed in the following:

3.1 ERS scatterometer data

Coarse-resolution soil moisture data (25 km) were derived from backscatter measurements acquired with scatterometers on-board of the European Remote Sensing (ERS) satellites ERS-1 and ERS-2, which operate in C-band. To retrieve the soil moisture, the method of Wagner et al. (1999) was used. The method exploits the multi-incidence angle observation capability of the sensor to account for seasonal changes in vegetation. The algorithm is a change detection approach, which scales the instantaneous backscatter measurement by dry and wet backscatter reference values derived from multi-year time series. This produces a scaled soil moisture index ranging from 0 to 1. These limits represent the minimum soil moisture (around the wilting point) and saturation, respectively. The retrieved information is hence a relative measure of the surface soil moisture content corresponding to the degree of saturation of the soil surface layer (< 2 cm). These data are the regional scale (coarse resolution) data to be downscaled.

3.2 ENVISAT ASAR data

The Advanced Synthetic Aperture Radar (ASAR) instrument onboard the European Environmental Satellite (ENVISAT) delivers radar data in C-band from 2002 to present. Data in Global Monitoring (GM) mode with a spatial resolution of 1 km were used here. The datasets were pre-processed in several steps: the data were geocoded and corrected for geometric distortions (Range Doppler approach) with the GTOPO30 digital elevation model (United States Geological Survey), together with Shuttle Radar Topography Mission (SRTM)

data. The radiometric calibration corrected for the scattering area, antenna gain pattern and range spread loss. To account for the differences due to varying incidence angles and distances from the sensor, the data were normalised to a reference angle. These data are the local scale (high resolution) data used to test the plausibility of the downscaling method.

3.3 Soil information data

The European Soil Database (ESDB) contains soil related parameters for Europe with a cell size of 1 km x 1 km (version 2), and is available from the Joint Research Centre (JRC) of the European Commission. Soil texture and soil depths were used here.

3.4 Digital terrain data

The GTOPO30 digital elevation model was used in this study. GTOPO30 is a global digital elevation model (DEM) resulting from a collaborative effort led by U.S. Geological Survey's EROS Data Center. Elevations in GTOPO30 are regularly spaced at 30-arc seconds (approximately 1 kilometre in Europe).

3.5 Precipitation data

Spatial patterns of mean annual precipitation in Europe from the WorlClim database (http://www.worldclim.org/) were used in this study. WorldClim is a set of global climate layers (climate grids) with a spatial resolution of a square kilometre. Although the precipitation data are not very accurate over the Alps, they were used here to demonstrate the feasibility of the approach.

4. Results

4.1 Fingerprints

Figures 5 – 8 show the fingerprints obtained with the parameters of Table 1 and the data summarised in section 3 of this report. In all the figures, red relates to low values of the fingerprints and blue relates to large values. This means that the red pixels will contribute to small values of local soil moisture, provided the process is considered to be operative in this pixel according to Table 1. Similarly, the blue pixels will contribute to large local soil moisture if applicable. The pattern of the ξ'_1 fingerprint in Figure 5 represents the saturation excess runoff generation process controlled by mean annual precipitation and terrain curvature. The mountain ranges feature large local soil moisture values because of generally high precipitation and large curvatures in the valleys. The pattern of the ξ'_{2a} and ξ'_{2b1} fingerprints in Figure 6 represents the infiltration excess runoff generation process controlled by soil texture. Red indicates coarse soils, blue indicates fine soils. In particular fluvial gravel deposits appear as coarse patterns in the map which will translate into low local soil moisture values. The pattern of the ξ'_{2b2} fingerprint in Figure 7 represents water logging or ponding processes controlled by terrain curvature. The difference between Figure 7 and Figure 5 illustrates the effect of precipitation on local soil moisture. The combined fingerprint ξ_L is shown in Figure 8. It has features of all components. The terrain characteristics are particularly visible. Part of the area such as former Yugoslavia has no data (shown as yellow), as no soil depth information was available in these areas. Figure 8 is the static fingerprint pattern ξ_L. The pattern could be straightforwardly extended to dynamic fingerprints if more information was available such as antecedent rainfall during the week before the soil moisture data were collected.

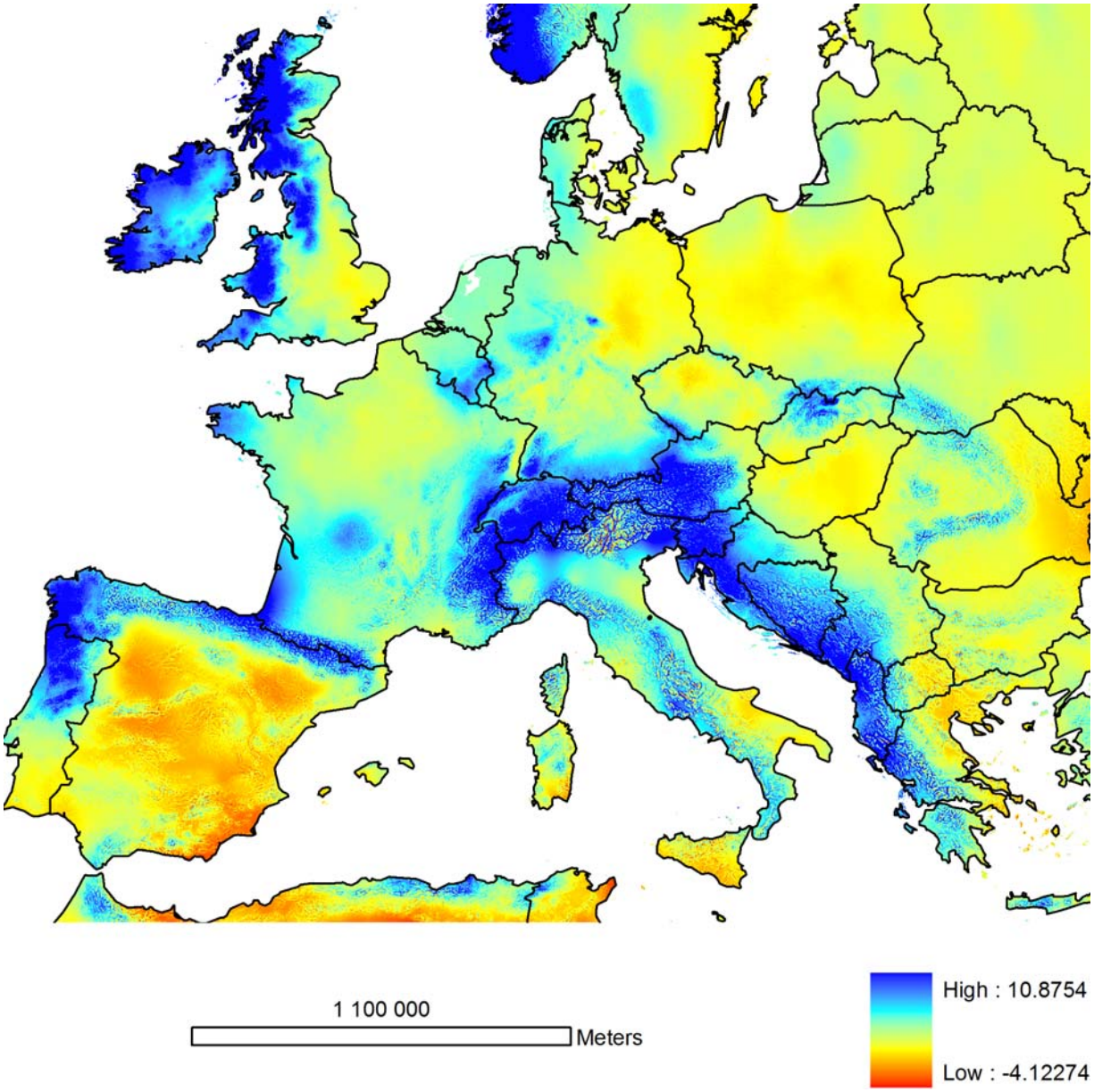

Figure 5: Pattern of the ξ'_1 fingerprint component representing saturation excess runoff generation processes related to lateral flow in the soil. Colour range is from red to blue.

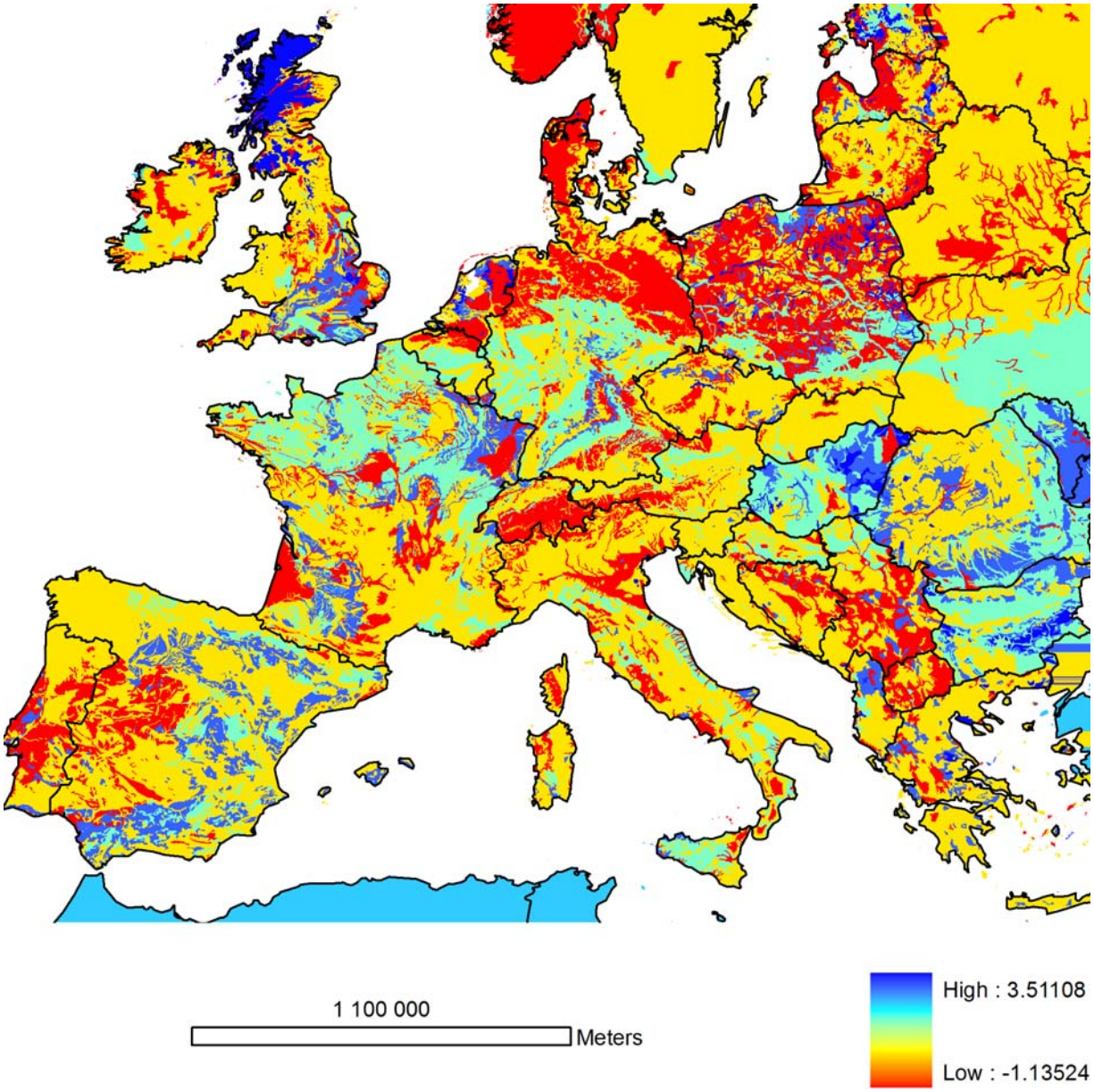

Figure 6: Pattern of the ξ'_{2a} and ξ'_{2b1} fingerprint components representing infiltration excess runoff generation processes related to vertical flow in the soil. Colour range is from red to blue, i.e., red indicates coarse soils, blue indicates fine soils.

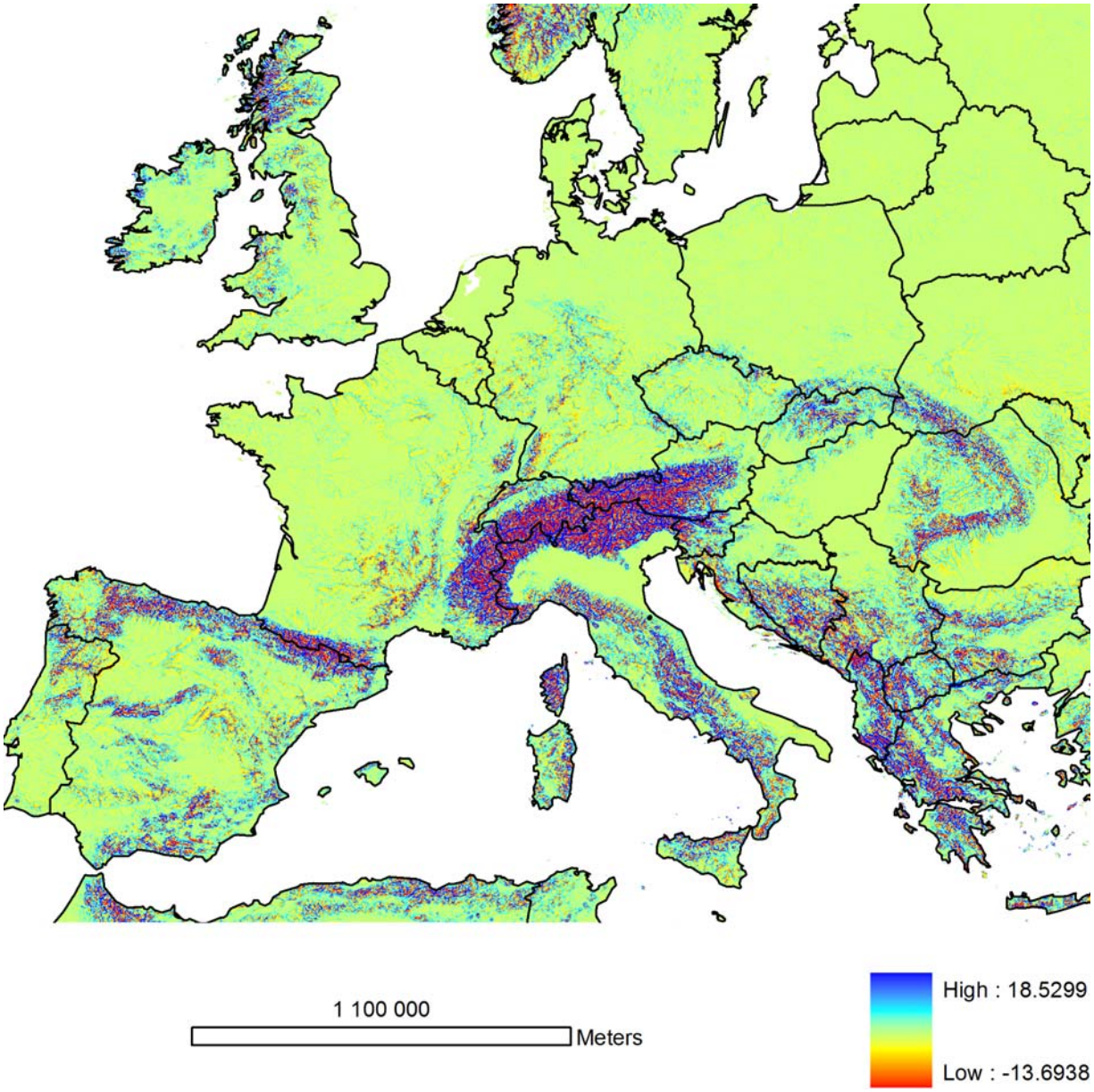

Figure 7: Pattern of the ξ'_{2b2} fingerprint component representing water logging or ponding processes when the groundwater table rises to the surface. Colour range is from red to blue.

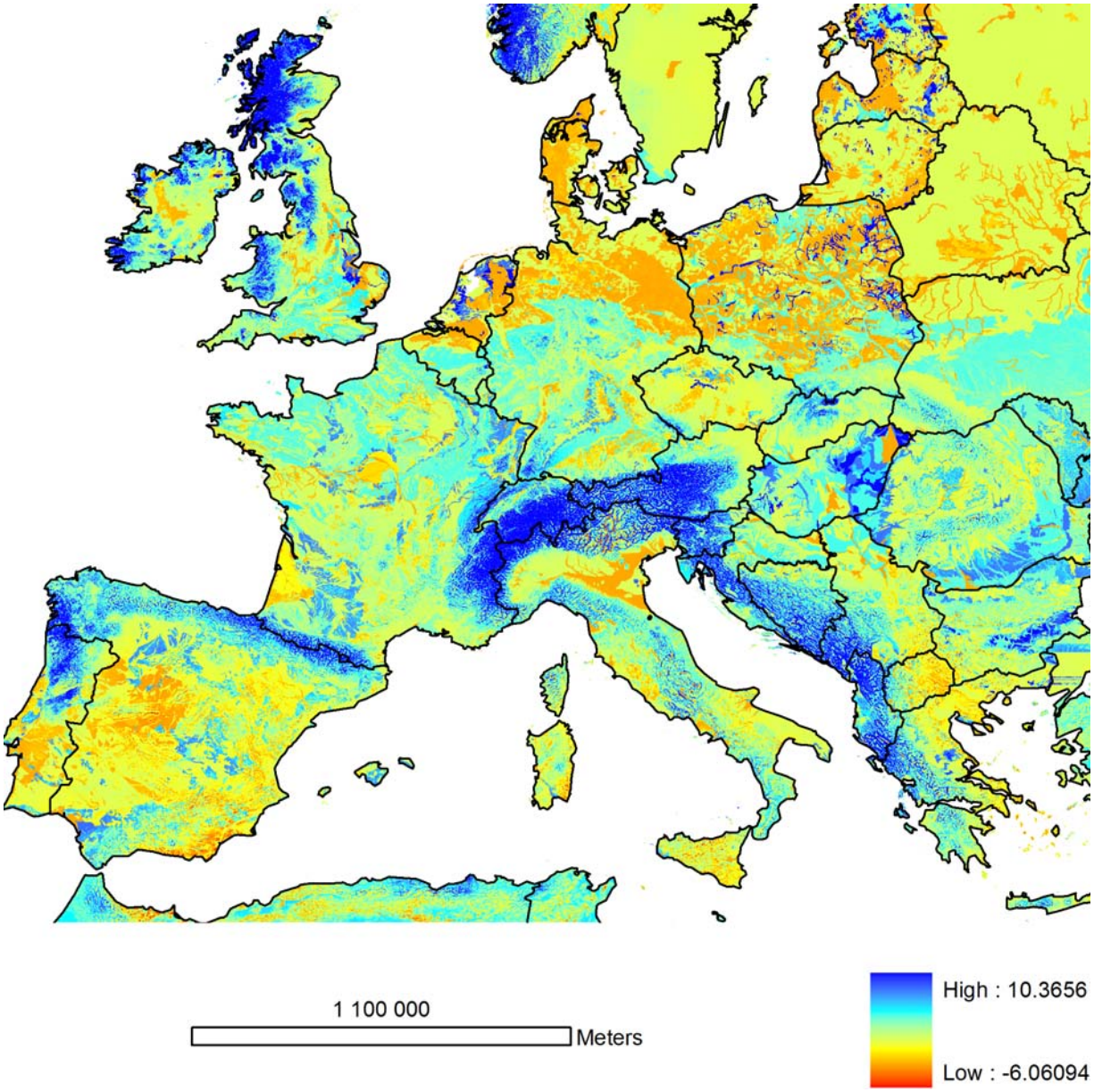

Figure 8: Pattern of the combined and normalised fingerprint ξ_L. Colour range is from red to blue.

4.2 Spatial variance for a random field

In order to test the downscaling model, a hypothetical large-scale soil moisture field Θ_R was generated by randomly drawing soil moisture values from a normal distribution with zero mean and unit variance. One such realisation has been used to calculate the large scale spatial standard deviation σ_R from subregions of 5x5 large-scale pixels. This means that the domain over which the standard deviation was calculated is 125 x 125 km which produces the rather smooth pattern in Figure 9. The small scale spatial standard deviation σ_L was then estimated from the large scale spatial standard deviation using scaling theory and is shown in Figure 10. The colour scales are not shown in the figure but the actual values of the local standard deviations in Figure 10 are about 80% larger than the regional standard deviations in Figure 9 because of the scale effect.

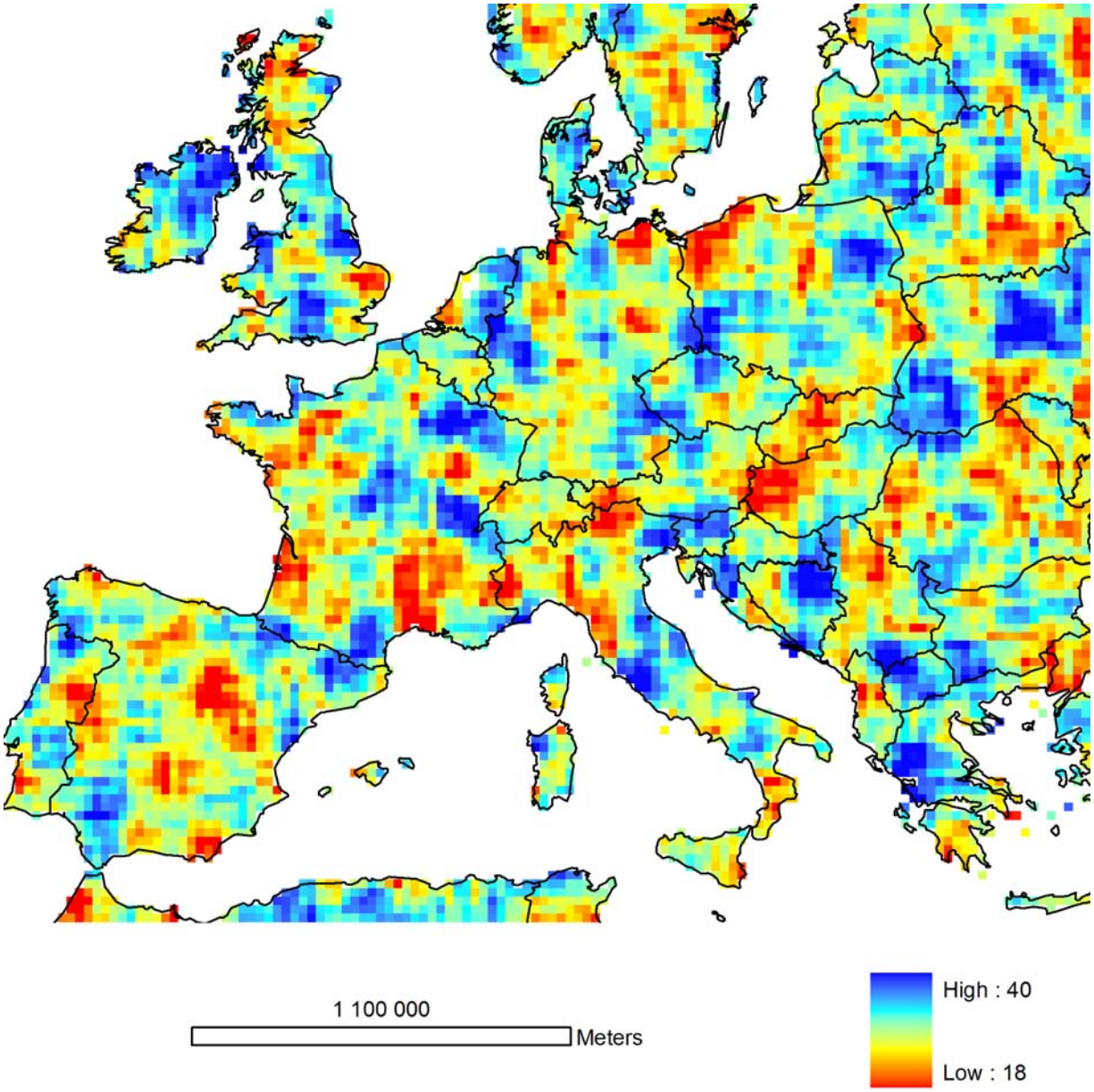

Figure 9: Large scale spatial standard deviation σ_R of soil moisture estimated from subregions of 5x5 large-scale pixels for a random field (see Figure 11). Colour range is from red to blue.

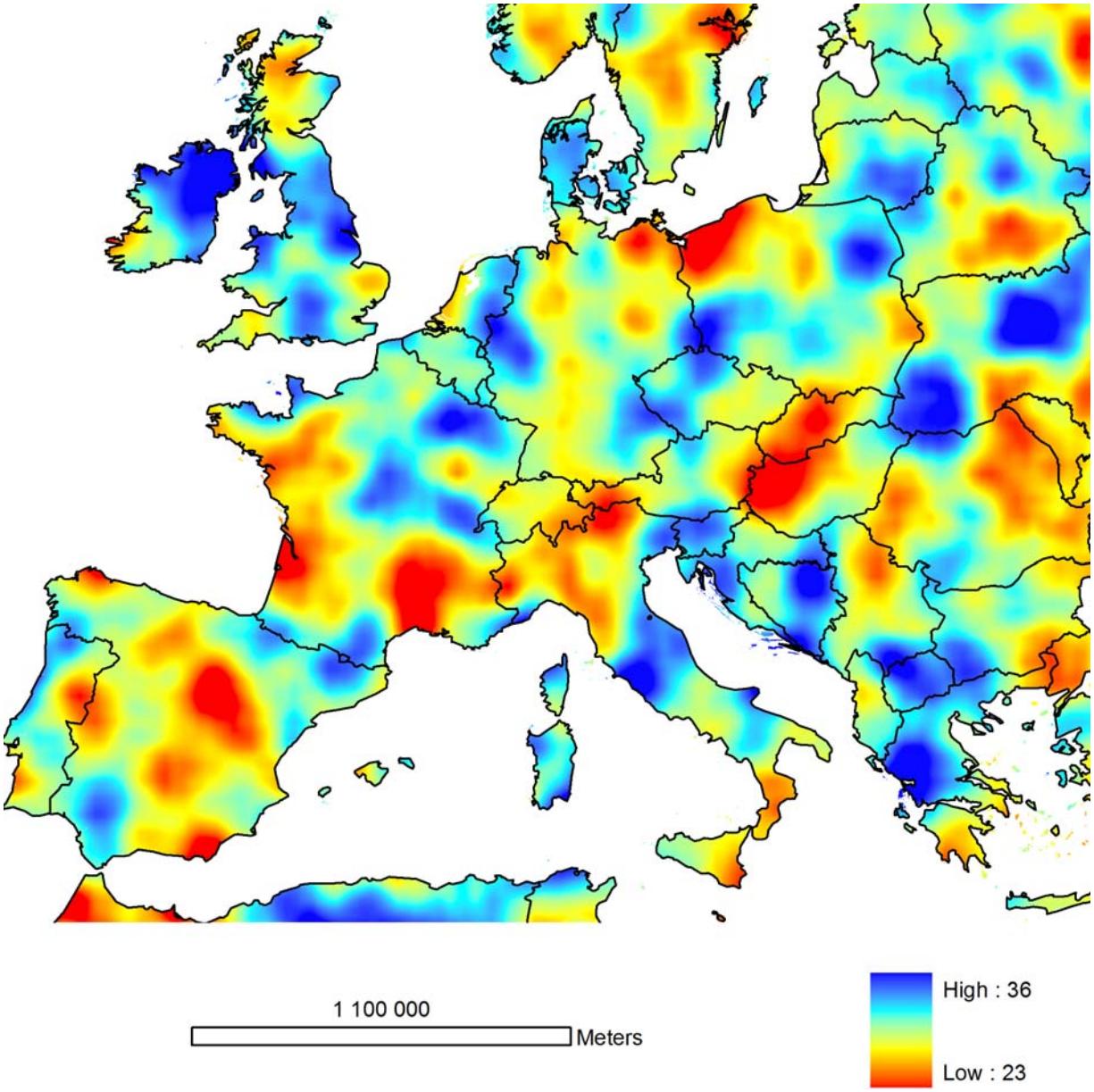

Figure 10: Small scale spatial standard deviation σ_L of soil moisture estimated from the large scale spatial standard deviation (Figure 9) using scaling theory. Colour range is from red to blue.

4.3 Downscaling results for a random field

As mentioned above, a hypothetical large-scale soil moisture field Θ_R was generated by randomly drawing soil moisture values from a normal distribution with zero mean and unit variance, in order to test the downscaling model. The realisation used in Figure 9 for calculating σ_R is shown in Figure 11. As the field was assumed to be fully random, no spatial correlations exist. This is a rigorous test of the downscaling method in terms of its spatial characteristics, as the spatial correlations present in the scatterometer data will lead to a more robust result than the one to be expected from a random field. Figure 12 shows the result of downscaling the random field. The spatial pattern is a mix of the large scale soil moisture imposed by Figure 11 and the fine scale pattern imposed by the fingerprint of Figure 8. It exhibits the spatial variance to be expected from the scaling theory and the spatial mean is consistent with that of the scatterometer data due to the unbiasedness constraint. The fine scale pattern of the downscaled image is related to topography, soils and climate as modelled by the hydrological process types of Figure 2. Some of the regular patterns at the large pixel scale present in Figure 11 are expected to disappear if the large scale pattern is autocorrelated as is the case with the scatterometer data.

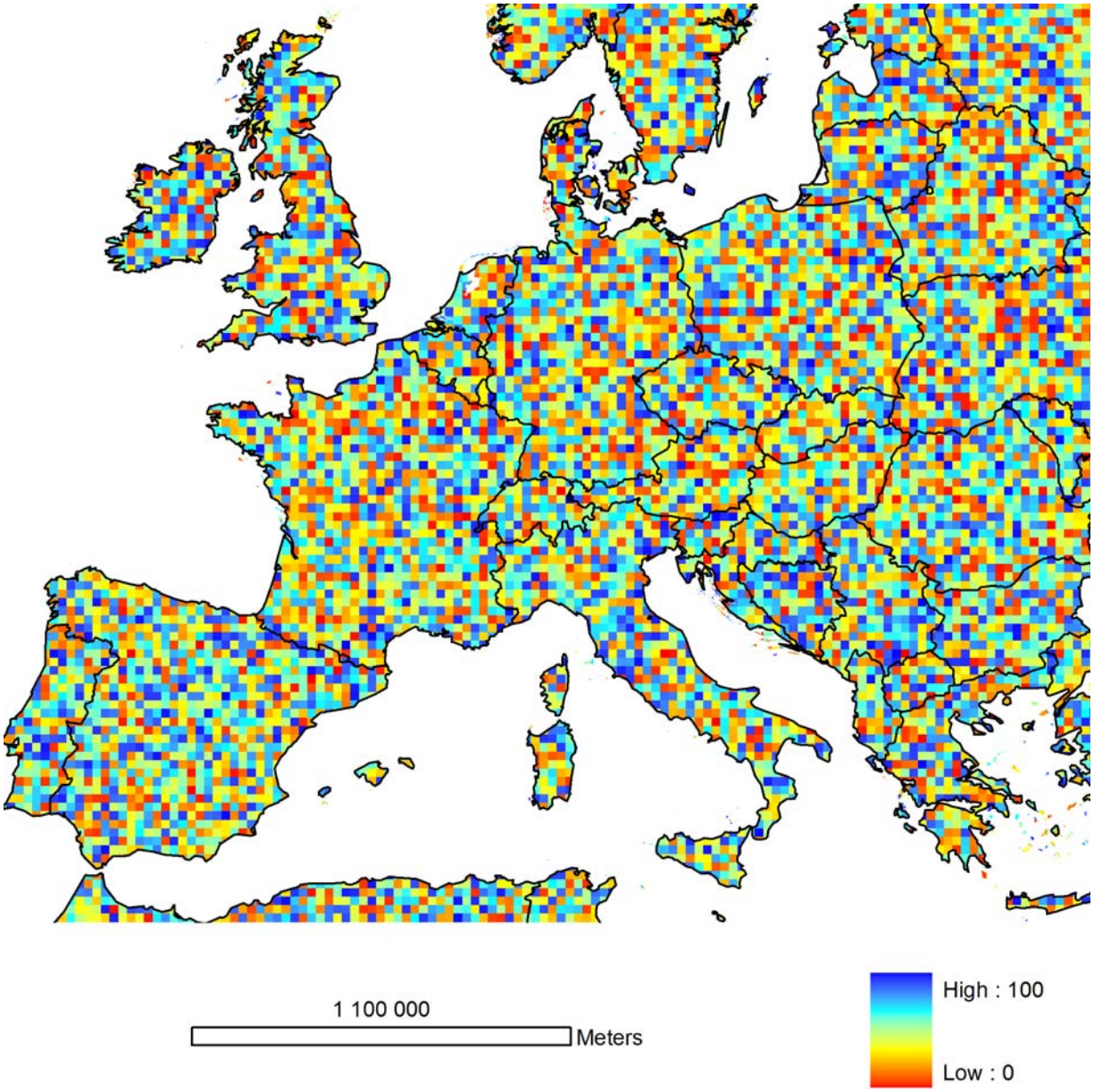

Figure 11: Random field of large scale soil moisture Θ_R. Colour range is from red to blue, i.e., red indicates dry soils, blue indicates wet soils.

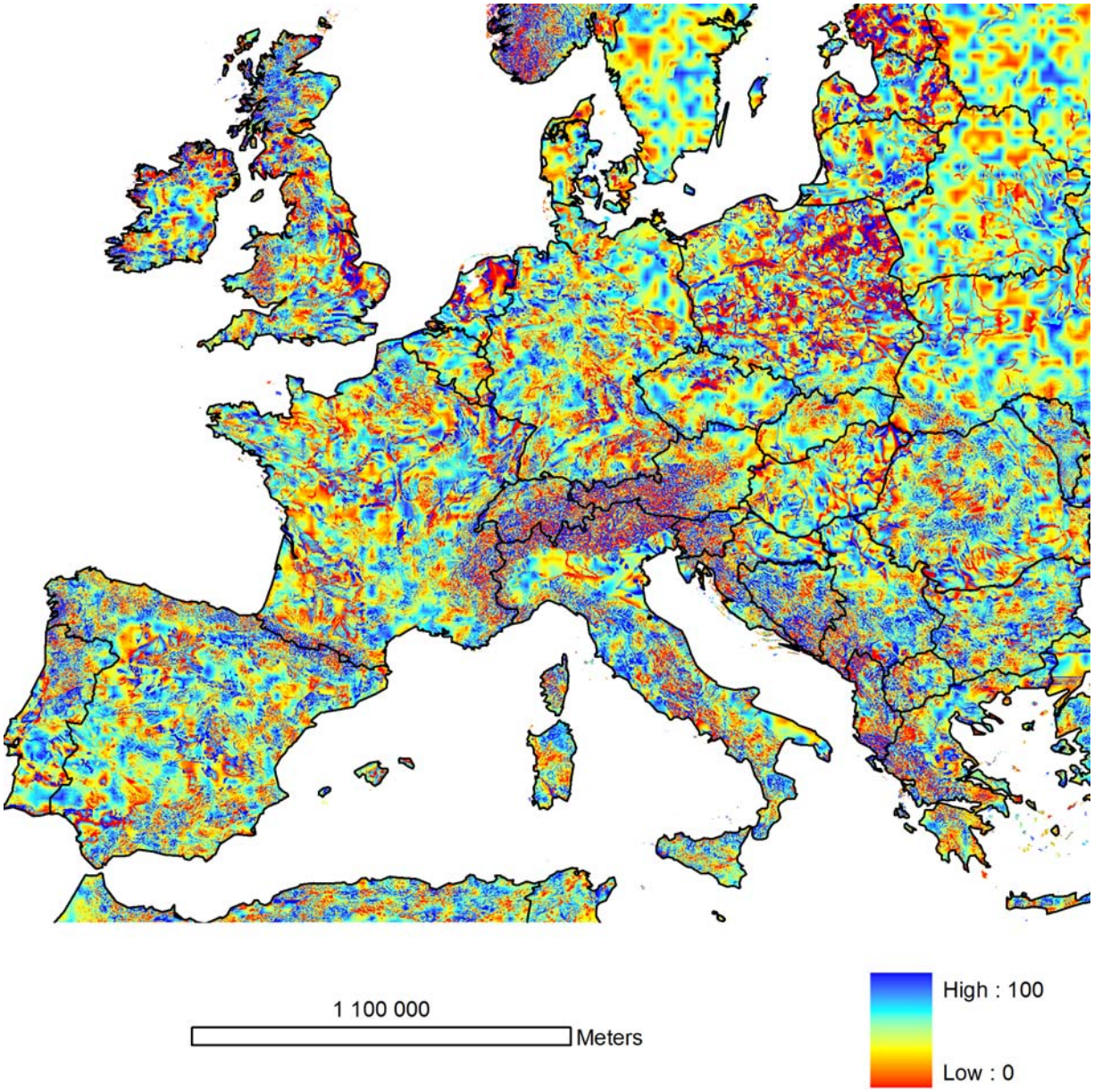

Figure 12: Small scale soil moisture Θ_L downscaled from Θ_R in Figure 11 using the hydrological downscaling approach. Colour range is from red to blue, i.e., red indicates dry soils, blue indicates wet soils.

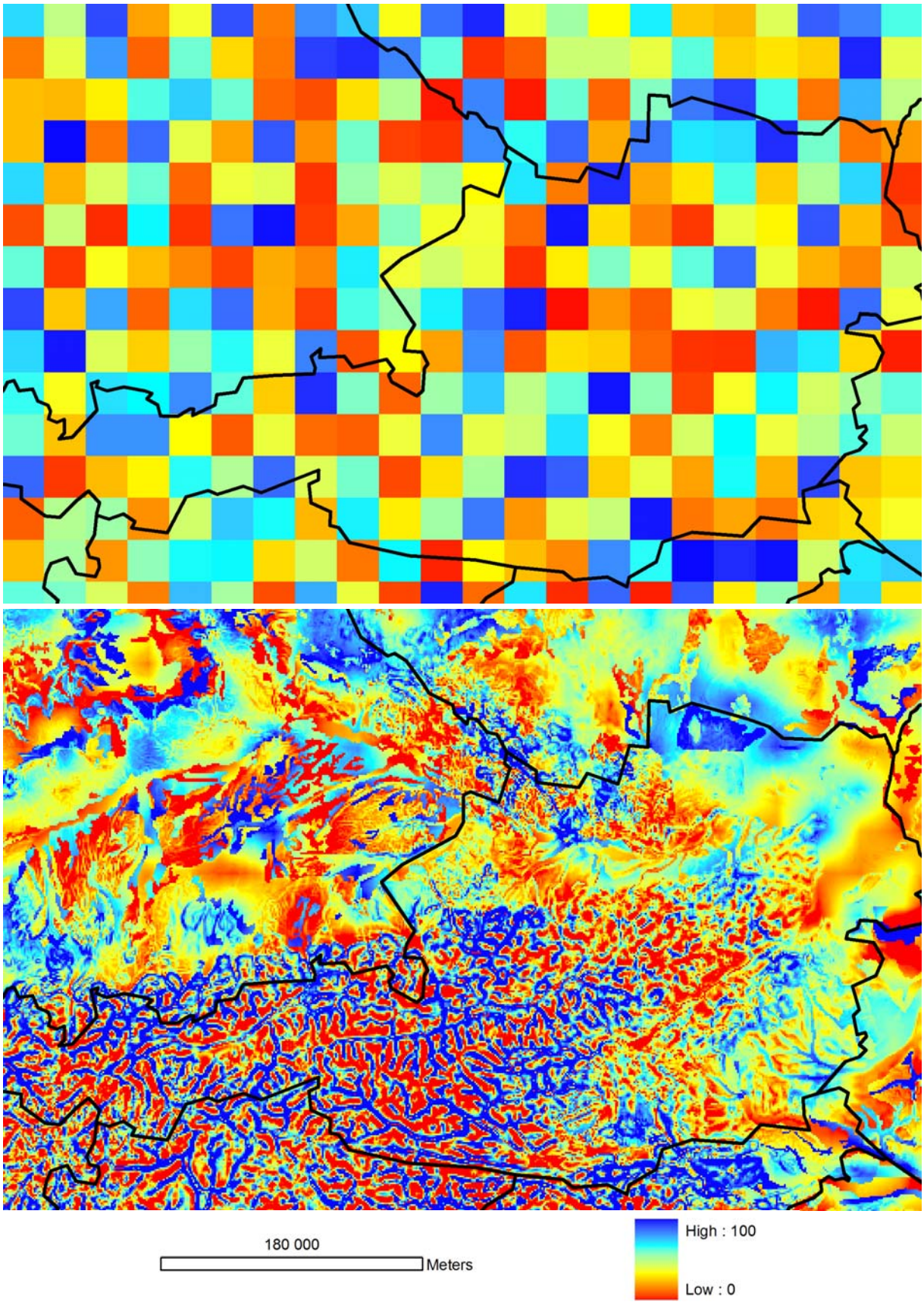

Figure 13: Details from Figures 11 and 12. Top: Random field of large scale soil moisture Θ_R. Bottom: Small scale soil moisture Θ_L downscaled from Θ_R. Colour range is from red to blue, i.e., red indicates dry soils, blue indicates wet soils. Map shows the Alpine range in the centre.

4.4 Downscaling results for scatterometer data

To demonstrate the feasibility of the hydrological downscaling approach it was applied to ERS scatterometer data. The downscaling approach was also tested for plausibility, so dates were selected when the downscaled soil moisture could be compared with ENVISAT data. While the ERS scatterometer data are at a resolution of about 25 km, the ENVISAT data are at a resolution of 1 km, so they allow an assessment of the downscaling method. However, the ENVISAT data are difficult to interpret quantitatively. The comparison should hence be viewed in terms of the spatial patterns rather than in quantitative terms.

To better assess the capabilities of the hydrological downscaling method, an alternative method was also applied in which the small-scale soil moisture field Θ_L was estimated from the large-scale soil moisture field Θ_R by adding random noise. The rationale of this is that this random downscaling method better represents the local scale variance than the original image but will not be able to represent the fine scale patterns. The comparison between the hydrological and random downscaling methods hence allows to assess the degree to which the hydrological approach can capture the fine scale patterns of soil moisture.

Figures 14 to 23 show the comparison of the methods. In each figure, (a) presents the regional-scale soil moisture field Θ_R based on the ERS scatterometer data; (b) presents a local-scale soil moisture field using the random downscaling; (c) presents the local-scale soil moisture field Θ_L using the hydrological downscaling; and (d) presents the ENVISAT data for comparison. Additionally, some of the figures show details of the Europe-wide images. As the dates have been selected to maximise the spatial match of the ERS scatterometer and the ENVISAT data, the distribution of the data within Europe is quite inhomogeneous.

Figures 14 to 23 suggest, that the hydrological downscaling indeed gives plausible results. The spatial pattern is a mix of the large scale soil moisture and the fine scale pattern imposed by the fingerprint of Figure 8. It exhibits the spatial variance to be expected from the scaling theory and the spatial mean is consistent with that of the scatterometer data due to the unbiasedness constraint. The fine scale pattern of the downscaled image is related to topography, soils and climate as modelled by the hydrological process types of Figure 2. The regular patterns at the large pixel scale present in Figure 11 indeed disappear since the large scale scatterometer data are autocorrelated in space.

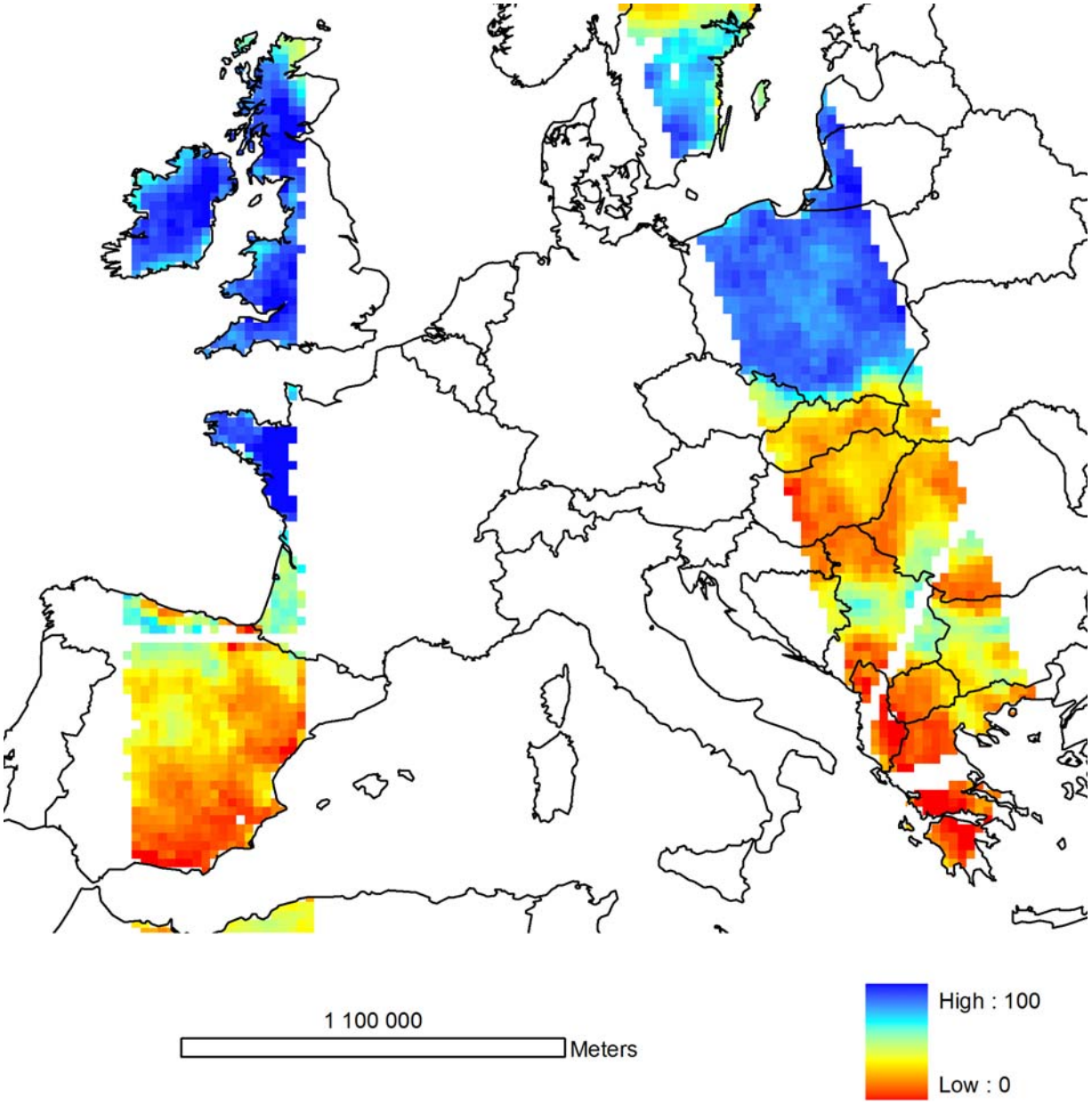

Figure 14a: Regional ERS scatterometer soil moisture – 2006-12-31

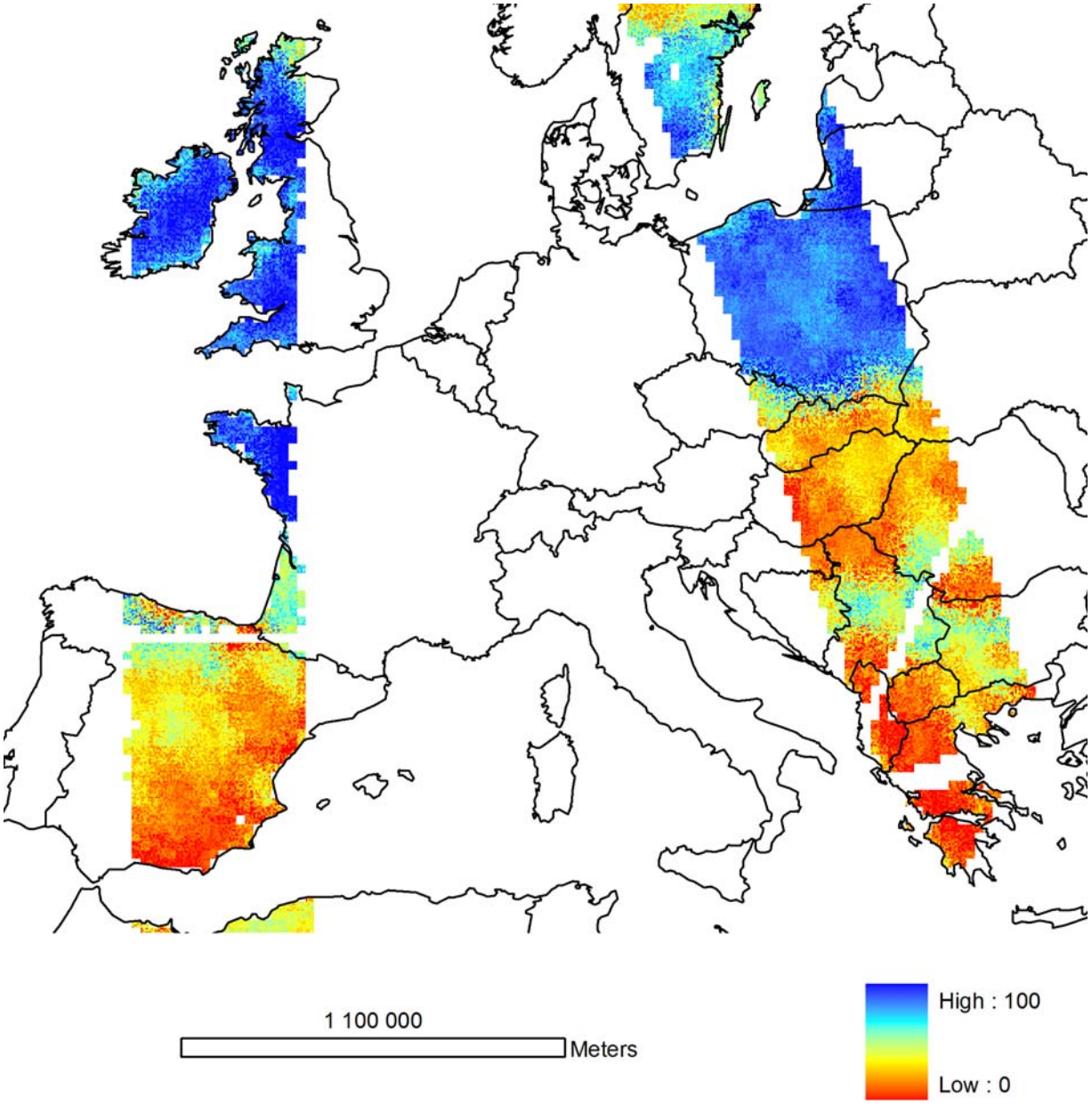

Figure 14b: Random downscaling - ERS scatterometer soil moisture – 2006-12-31

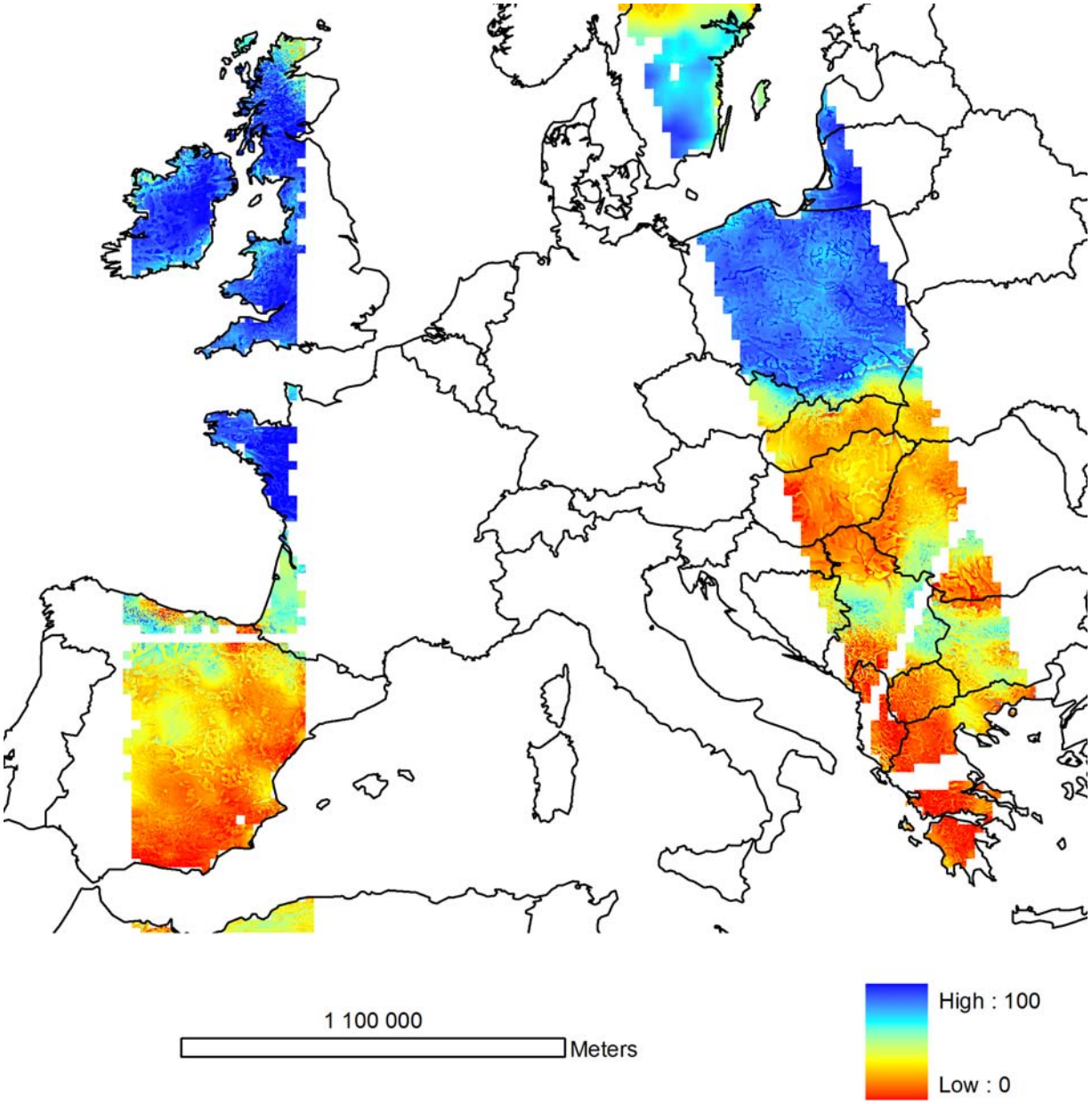

Figure 14c: Hydrological downscaling - ERS scatterometer soil moisture – 2006-12-31

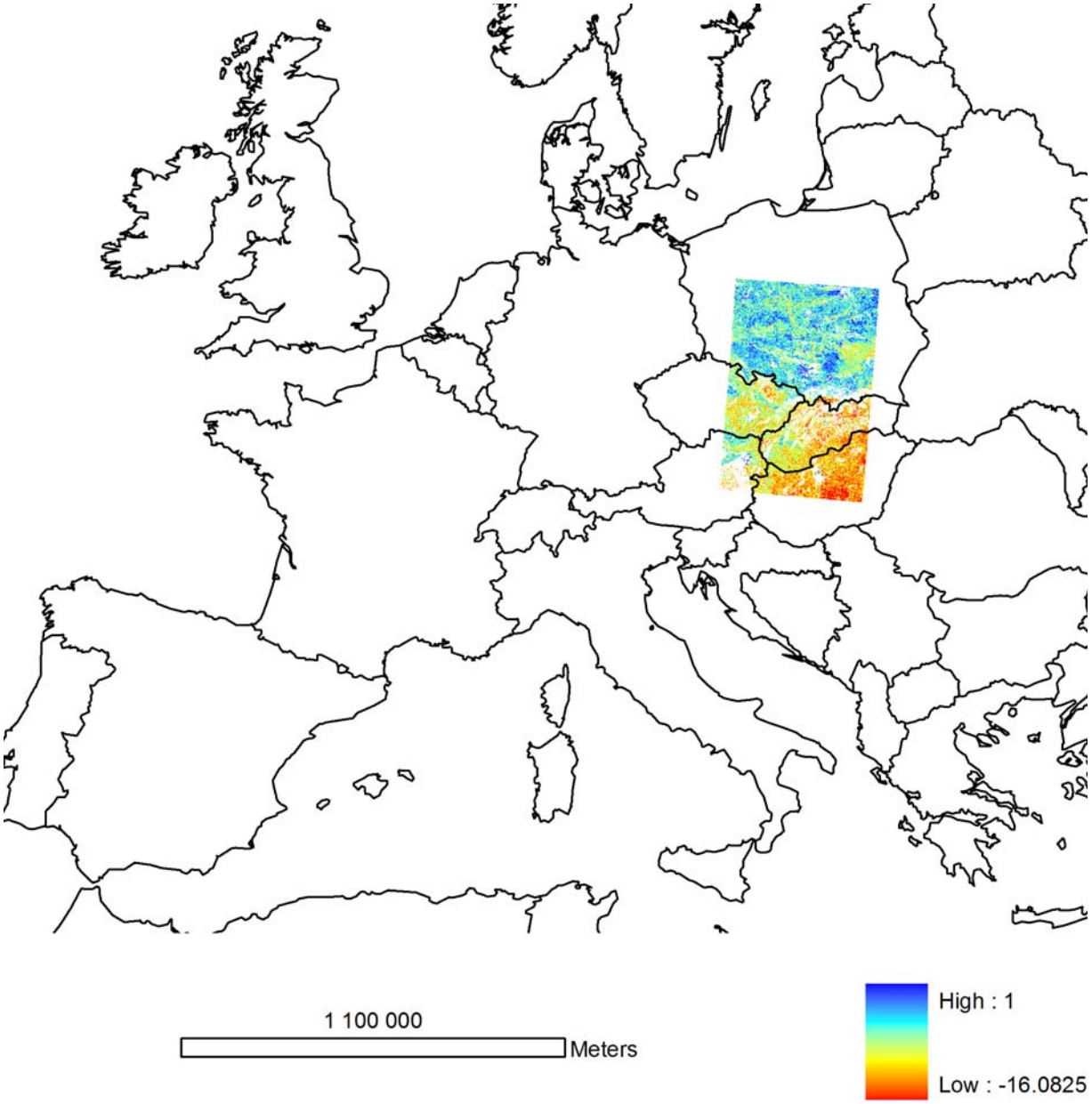

Figure 14d: Local ENVISAT soil moisture – 2006-12-31

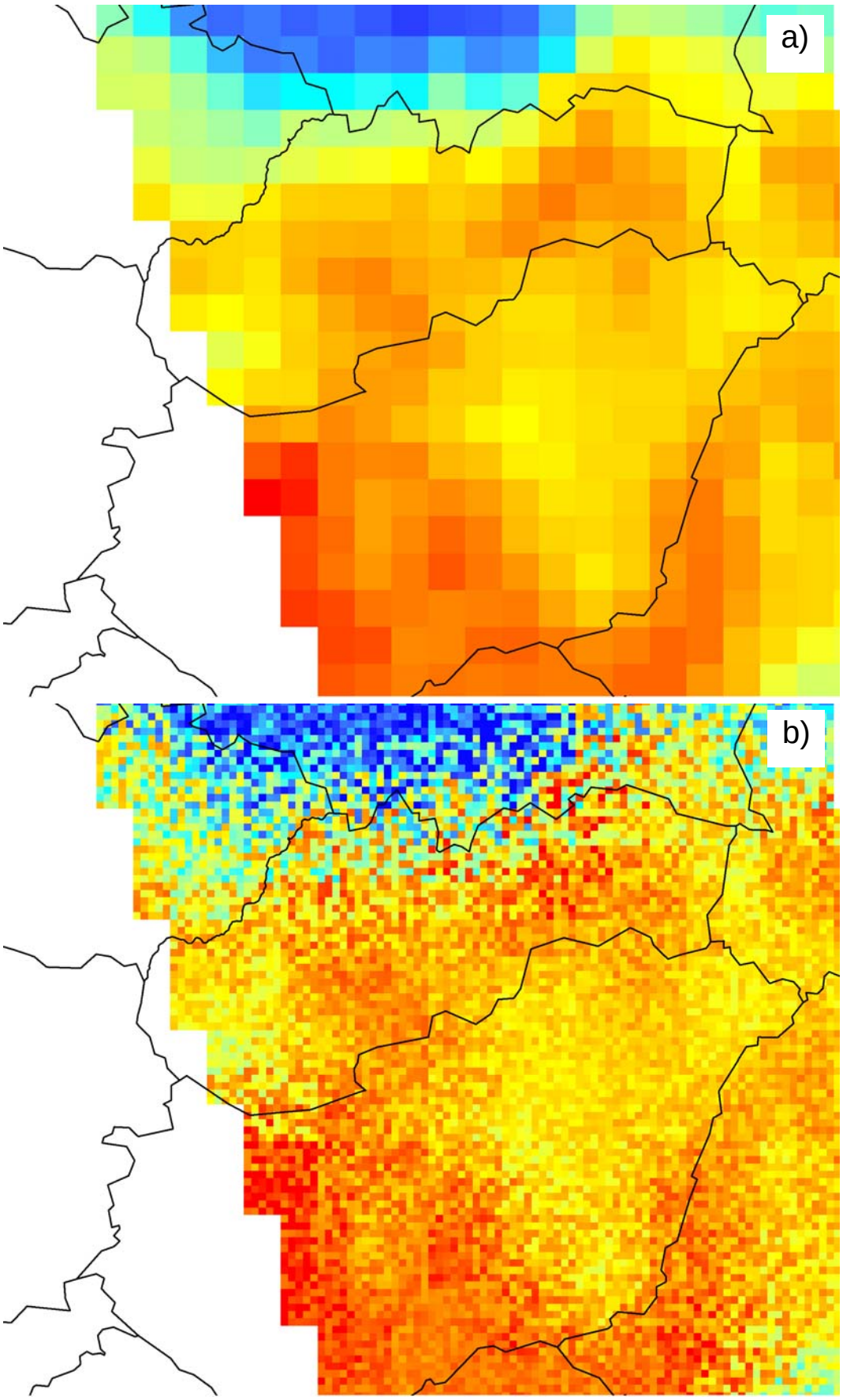

Figure 15: (a) Regional ERS scatterometer soil moisture, (b) Random downscaling – 2006-12-31 – detail Slovakia, Hungary

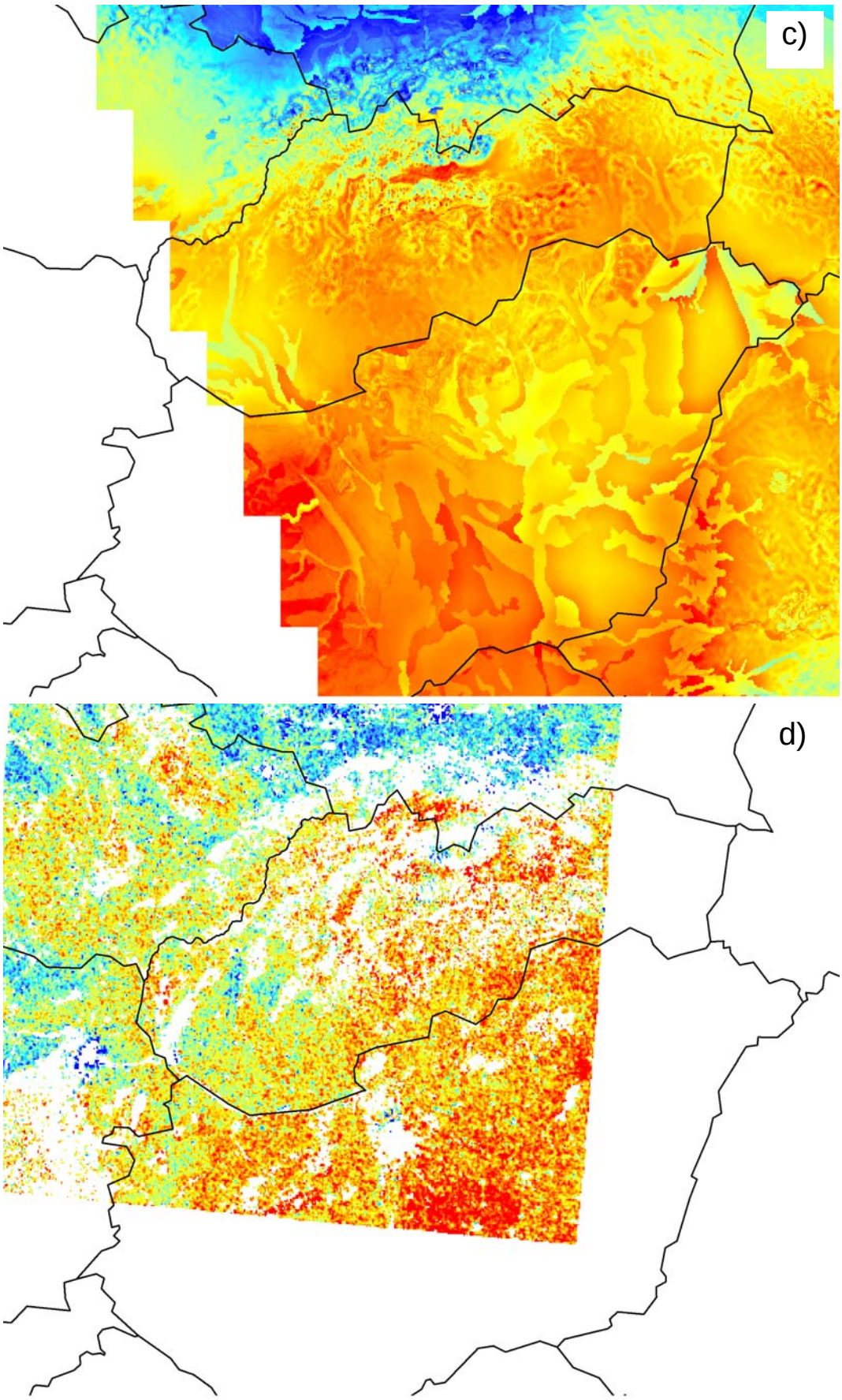

Figure 15: (c) Hydrological downscaling of ERS scatterometer soil moisture, (d) ENVISAT soil moisture – 2006-12-31 – detail Slovakia, Hungary

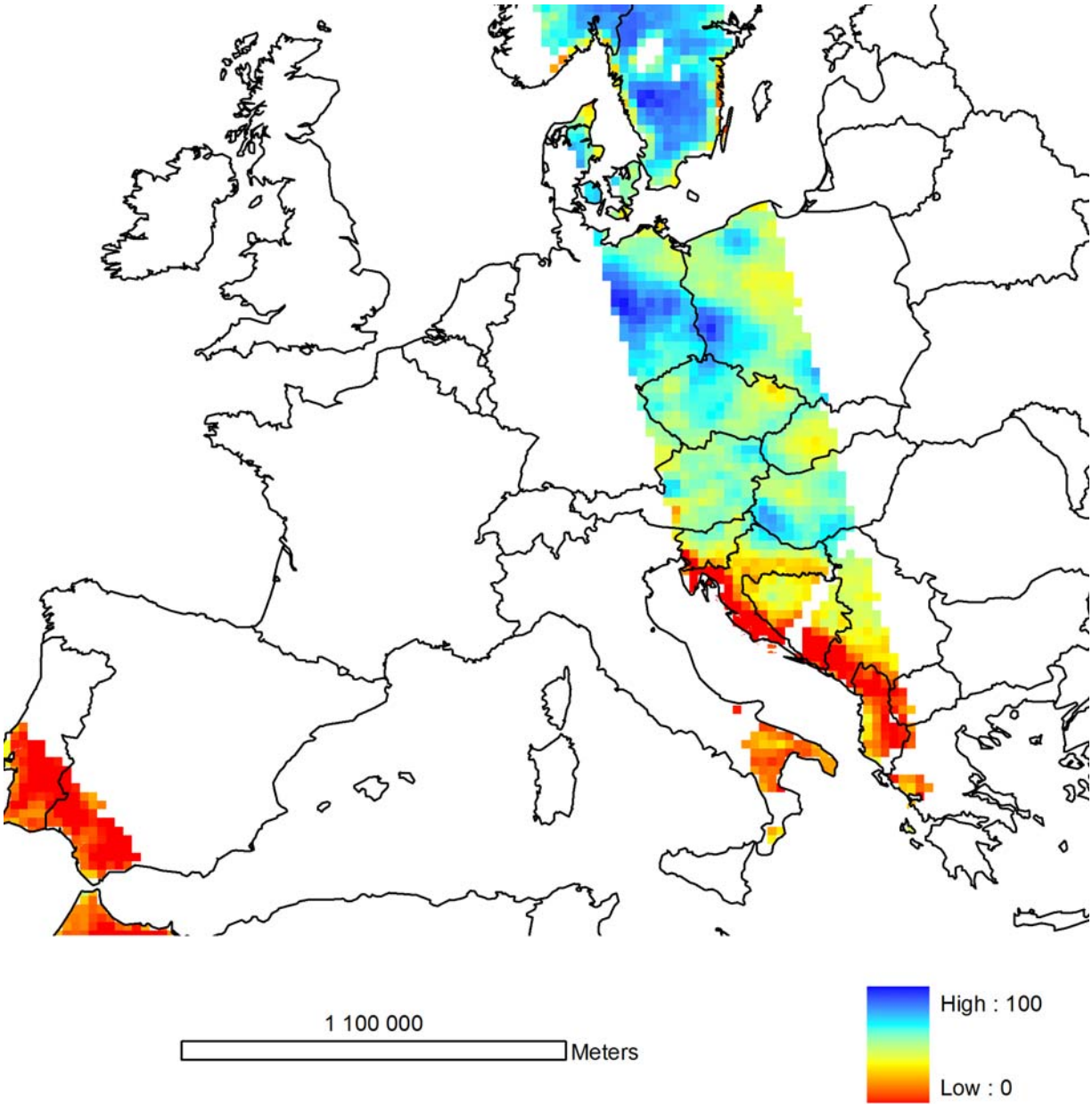

Figure 16a: Regional ERS scatterometer soil moisture – 2006-08-22

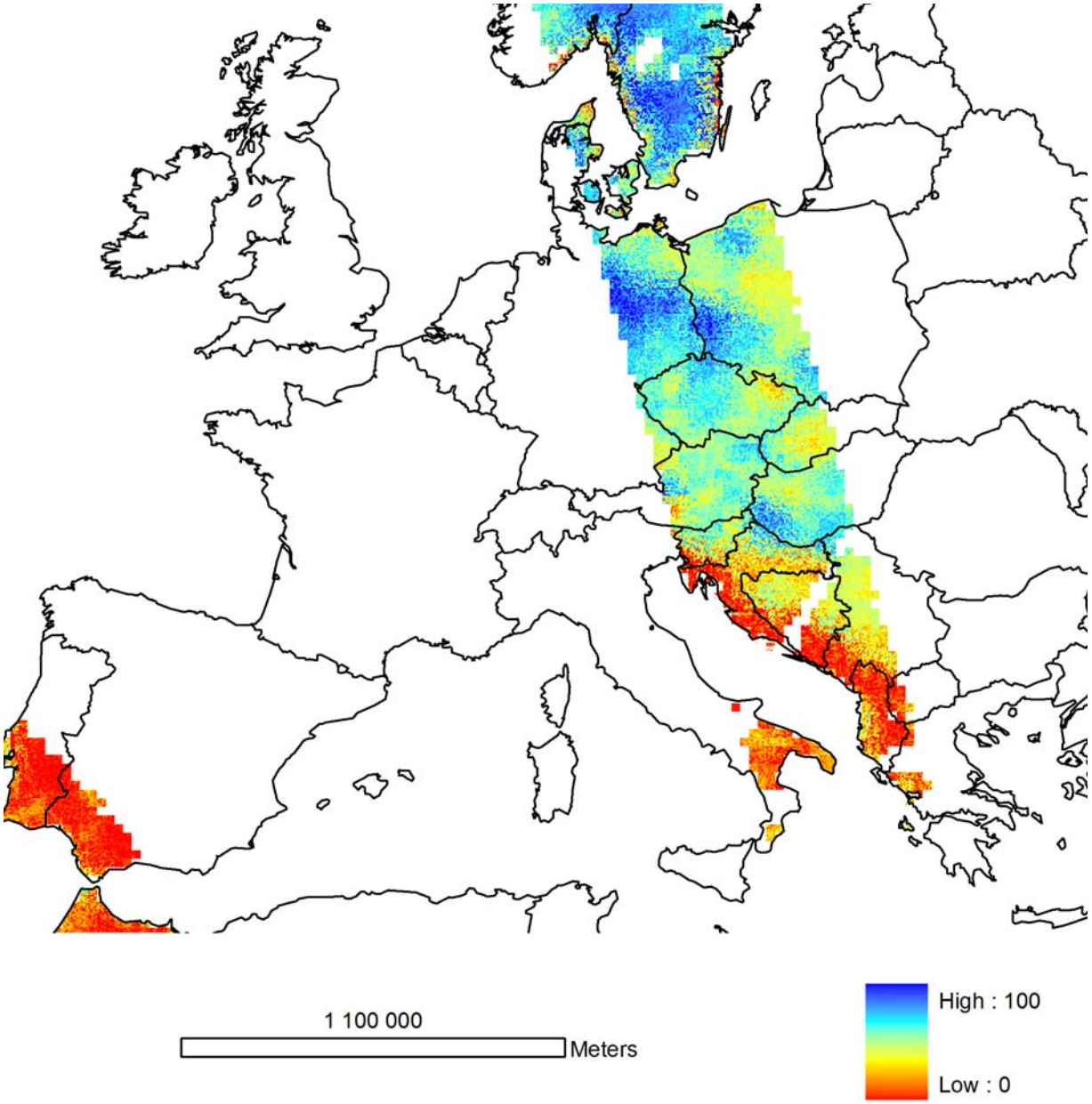

Figure 16b: Random downscaling - ERS scatterometer soil moisture – 2006-08-22

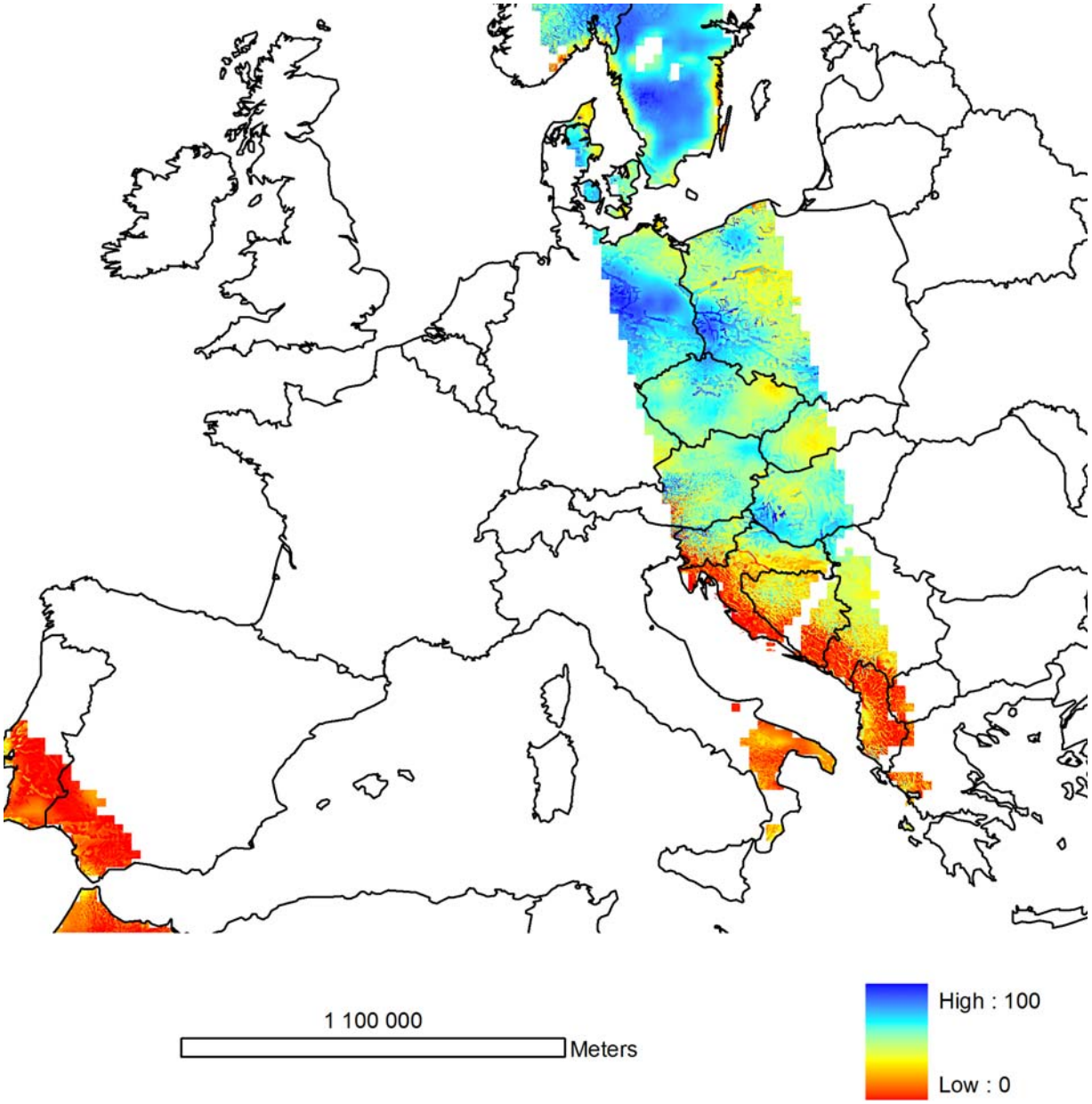

Figure 16c: Hydrological downscaling - ERS scatterometer soil moisture – 2006-08-22

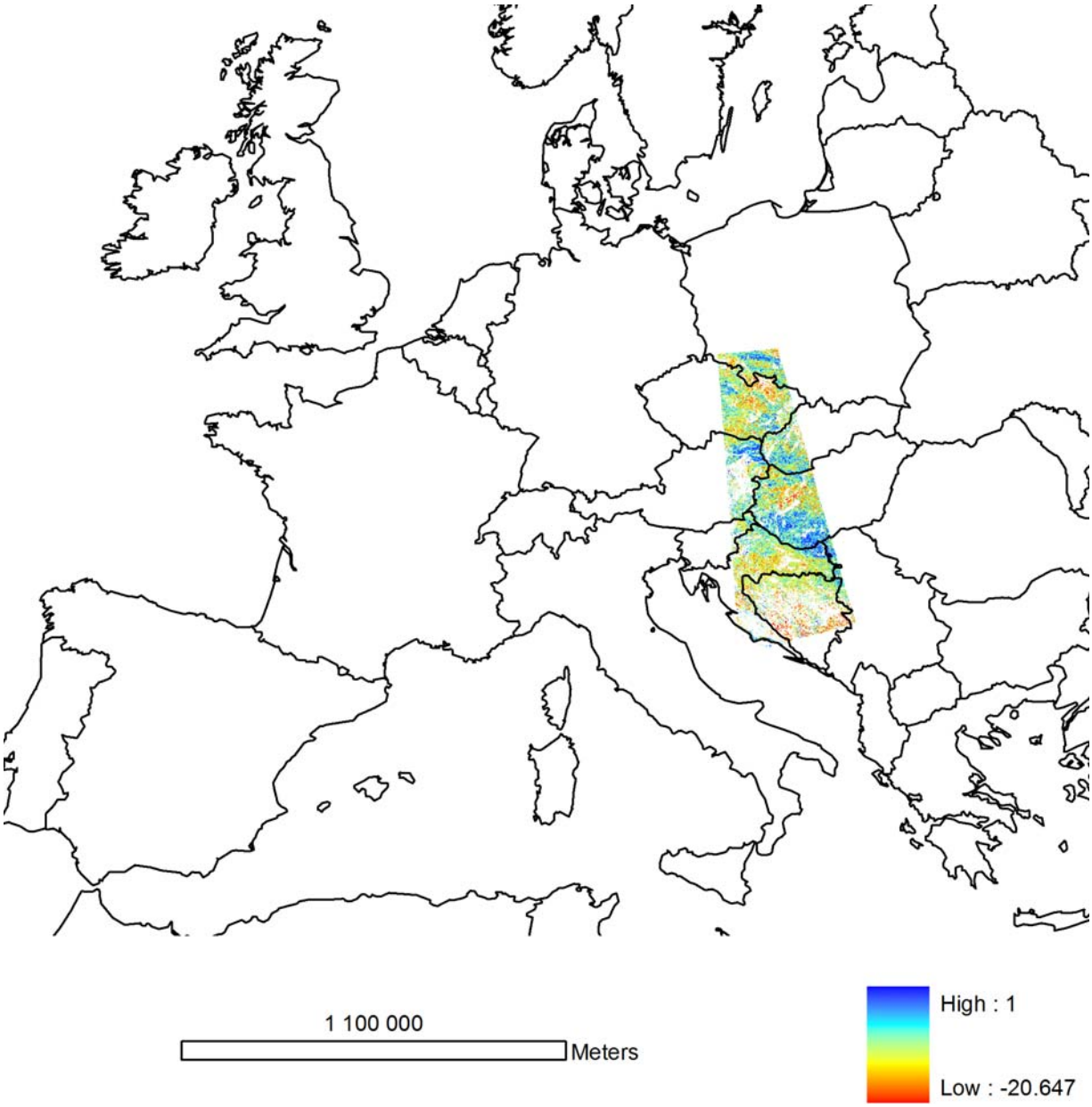

Figure 16d: Local ENVISAT soil moisture – 2006-08-22

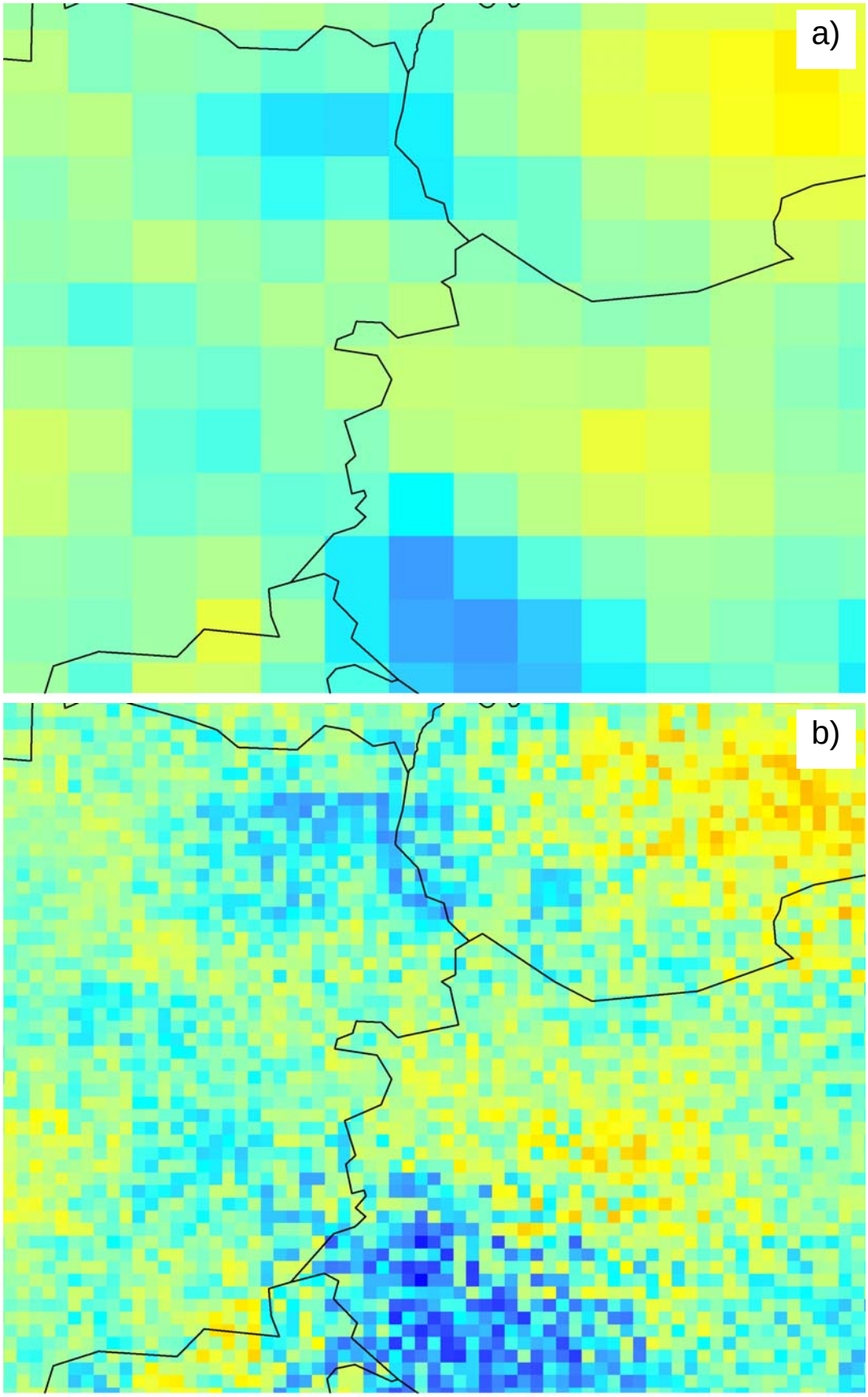

Figure 17: (a) Regional ERS scatterometer soil moisture, (b) Random downscaling – 2006-08-22– detail Austria, Hungary

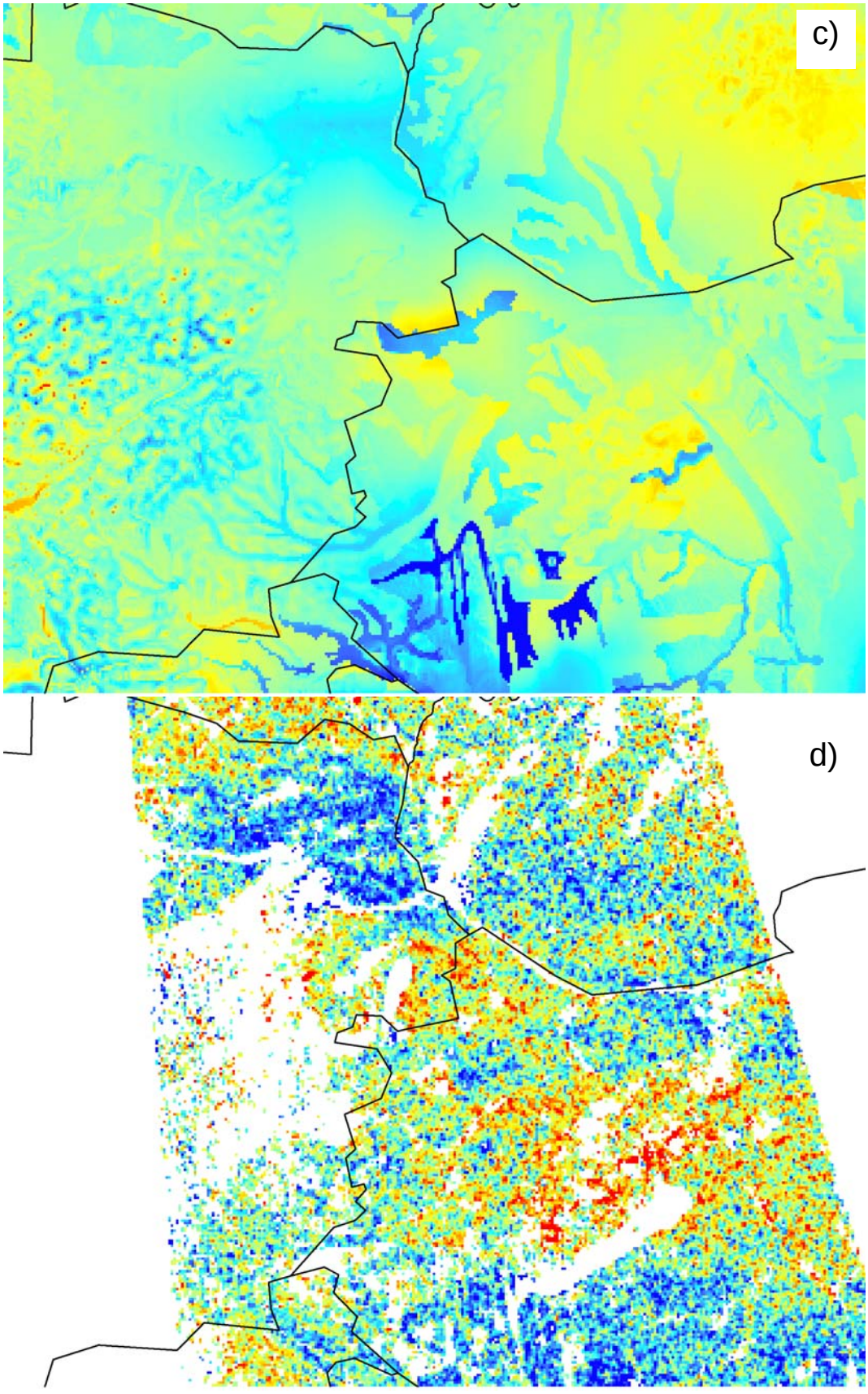

Figure 17: (c) Hydrological downscaling of ERS scatterometer soil moisture, (d) ENVISAT soil moisture – 2006-08-22– detail Austria, Hungary

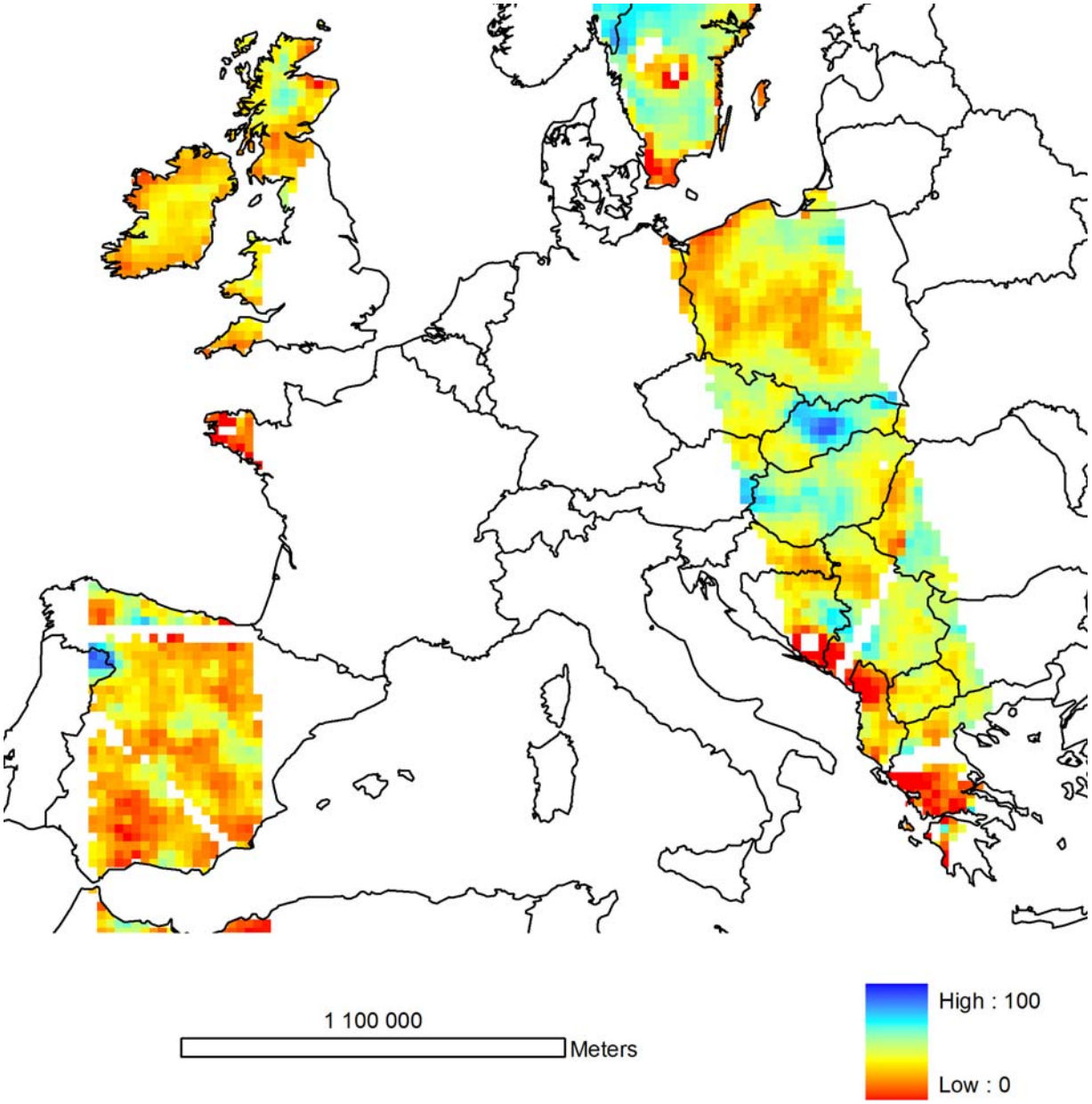

Figure 18a: Regional ERS scatterometer soil moisture – 2006-07-12

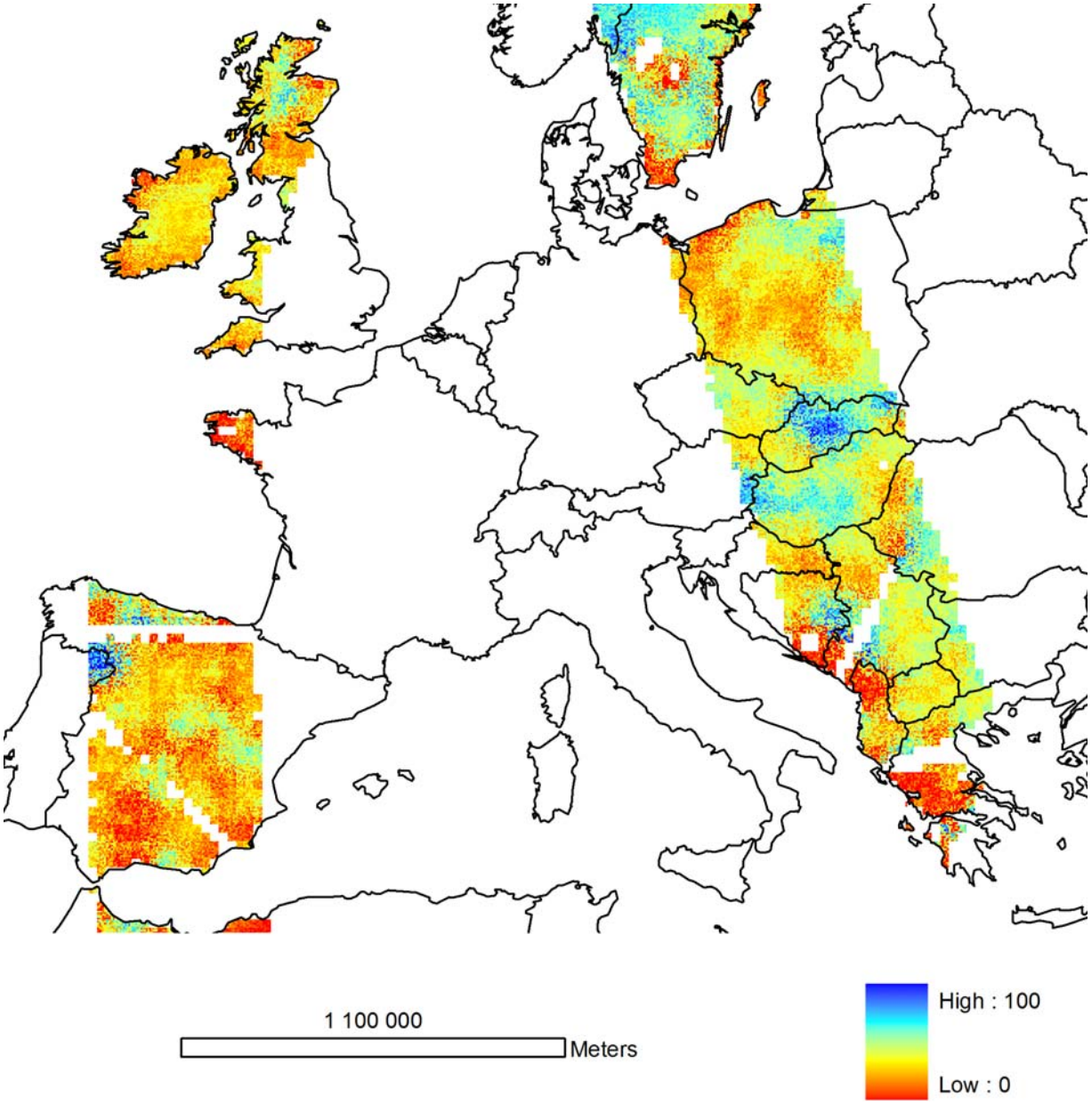

Figure 18b: Random downscaling - ERS scatterometer soil moisture – 2006-07-12

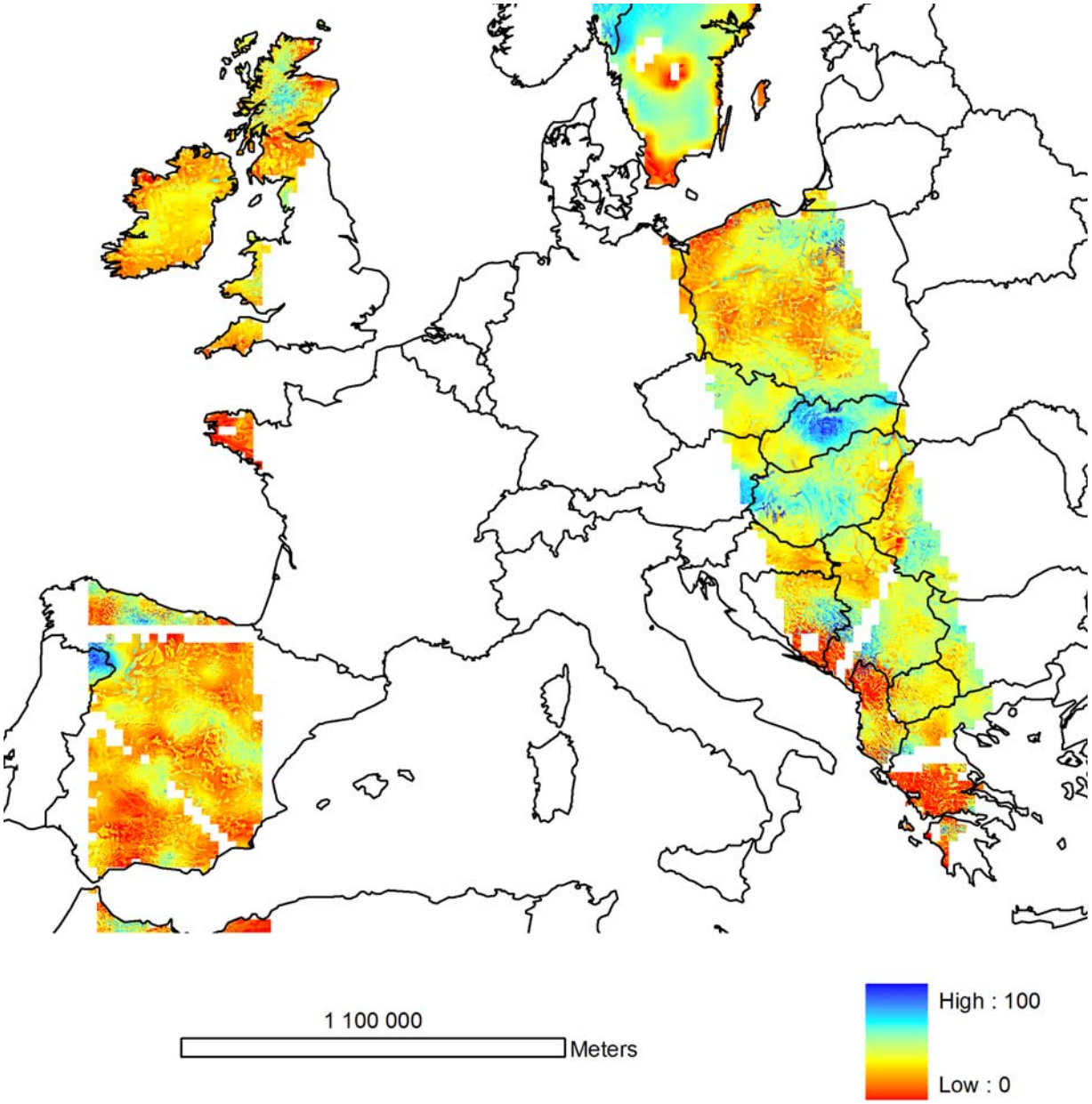

Figure 18c: Hydrological downscaling - ERS scatterometer soil moisture – 2006-07-12

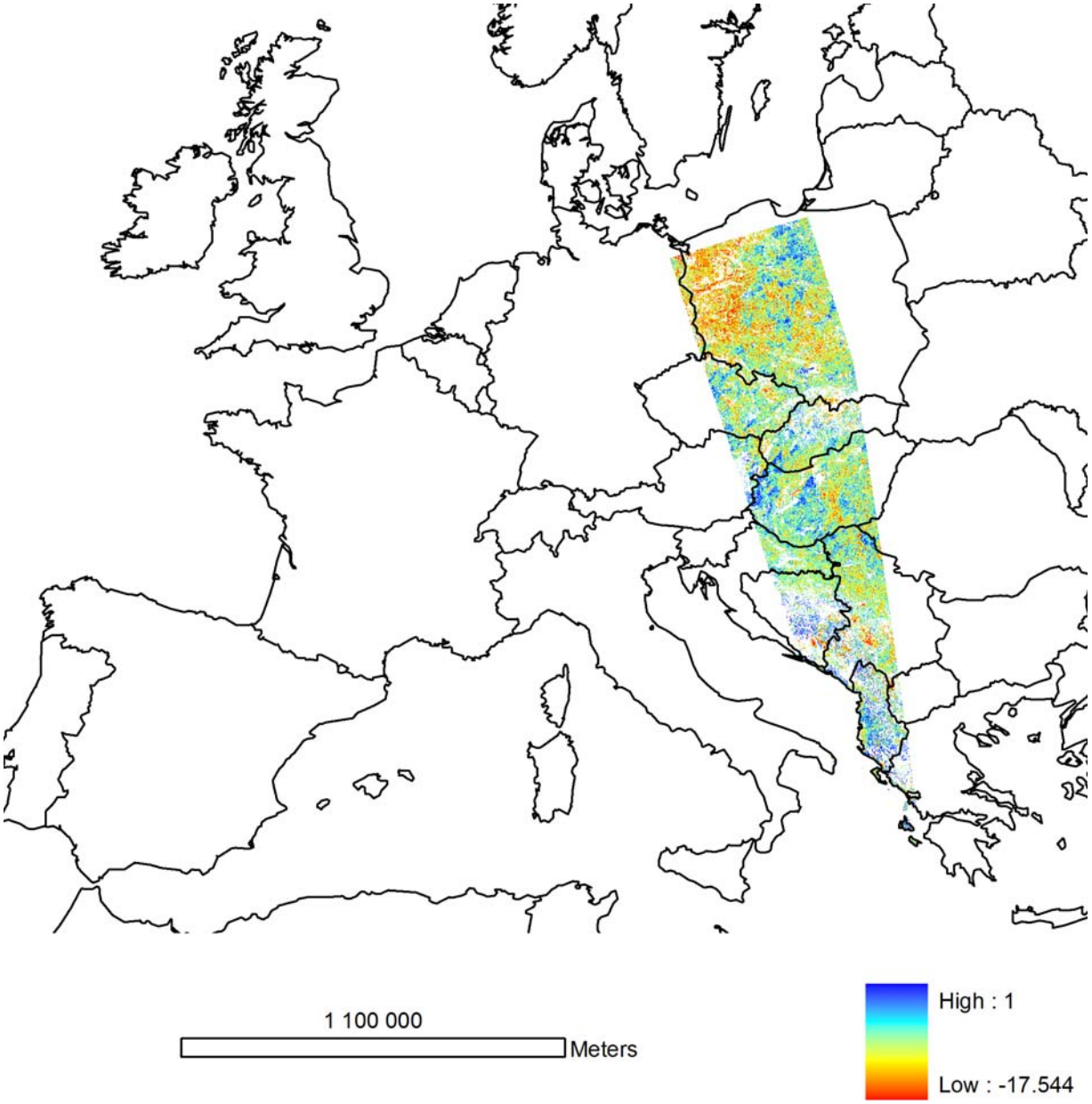

Figure 18d: Local ENVISAT soil moisture – 2006-07-12

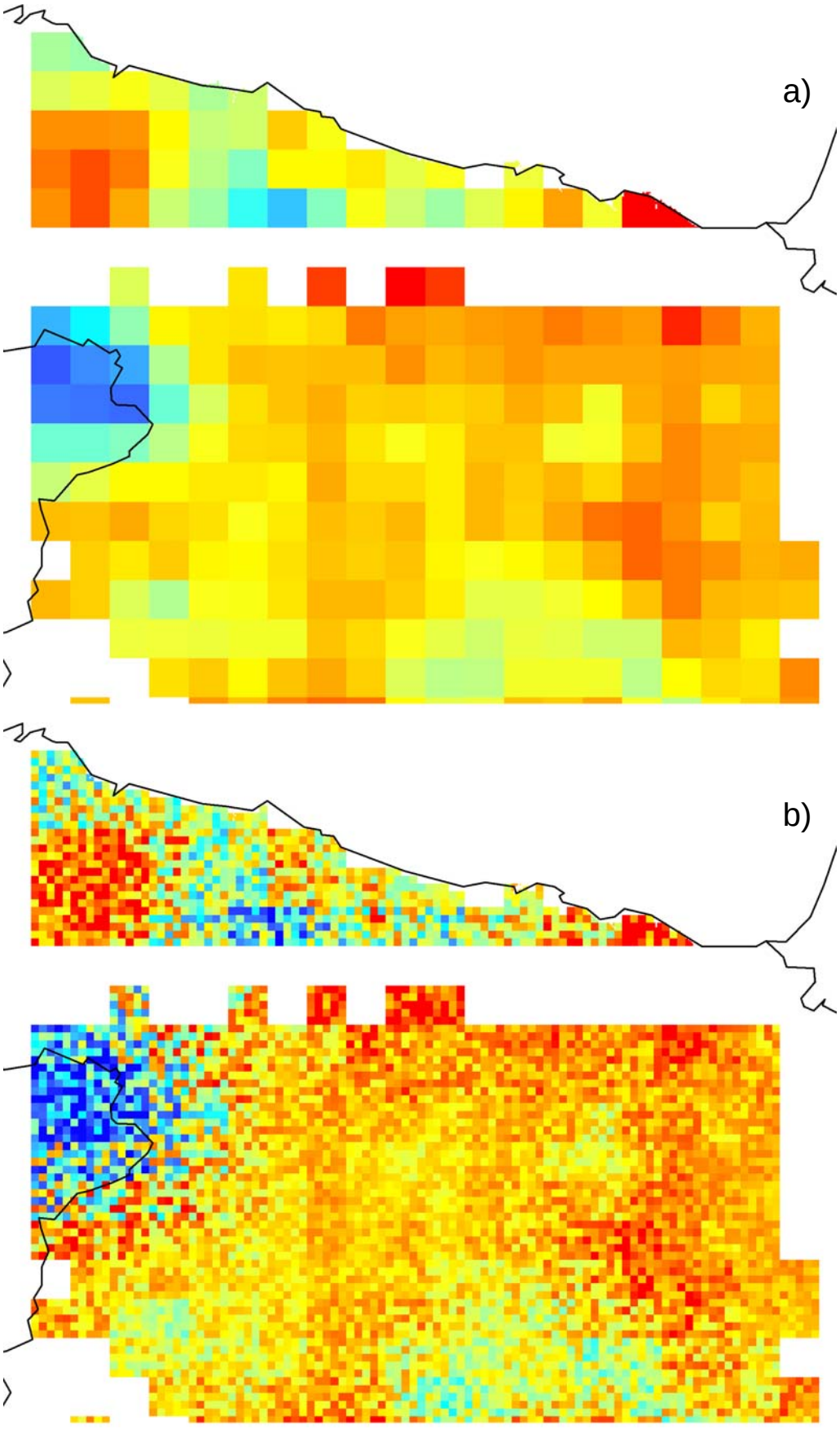

Figure 19: (a) Regional ERS scatterometer soil moisture, (b) Random downscaling – 2006-07-12 – detail Spain

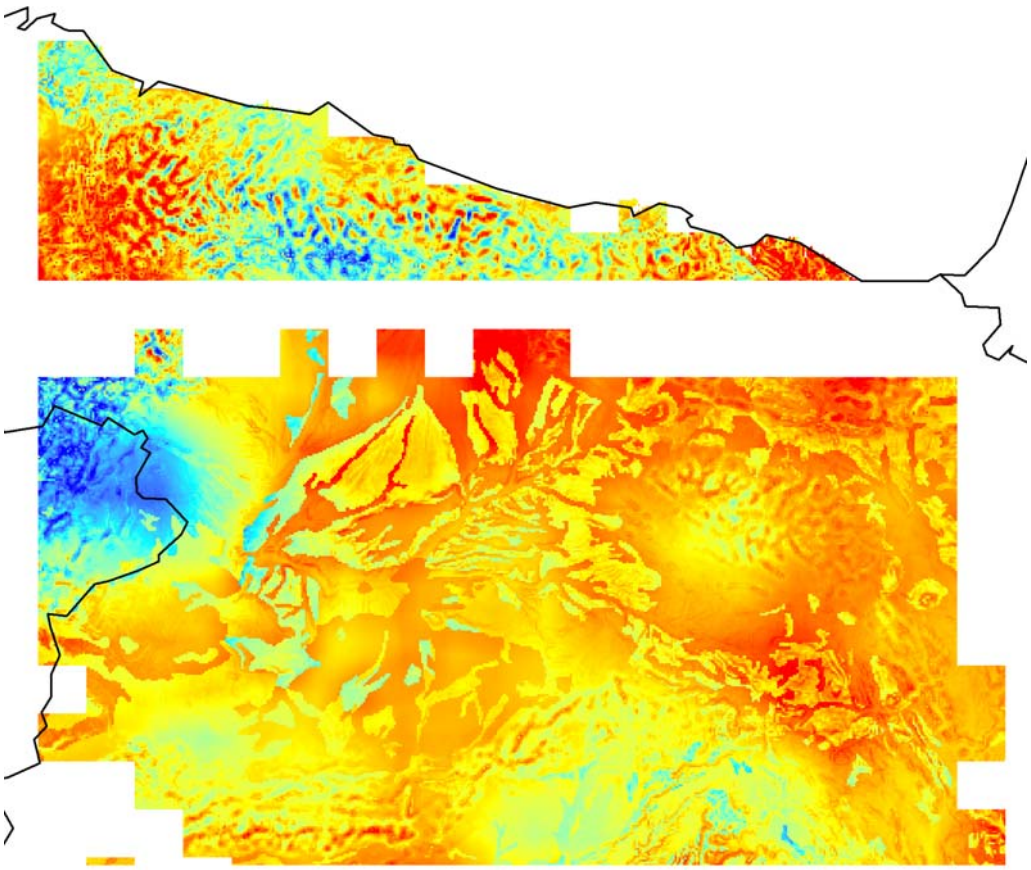

Figure 19c: Hydrological downscaling of ERS scatterometer soil moisture – 2006-07-12 – detail Spain

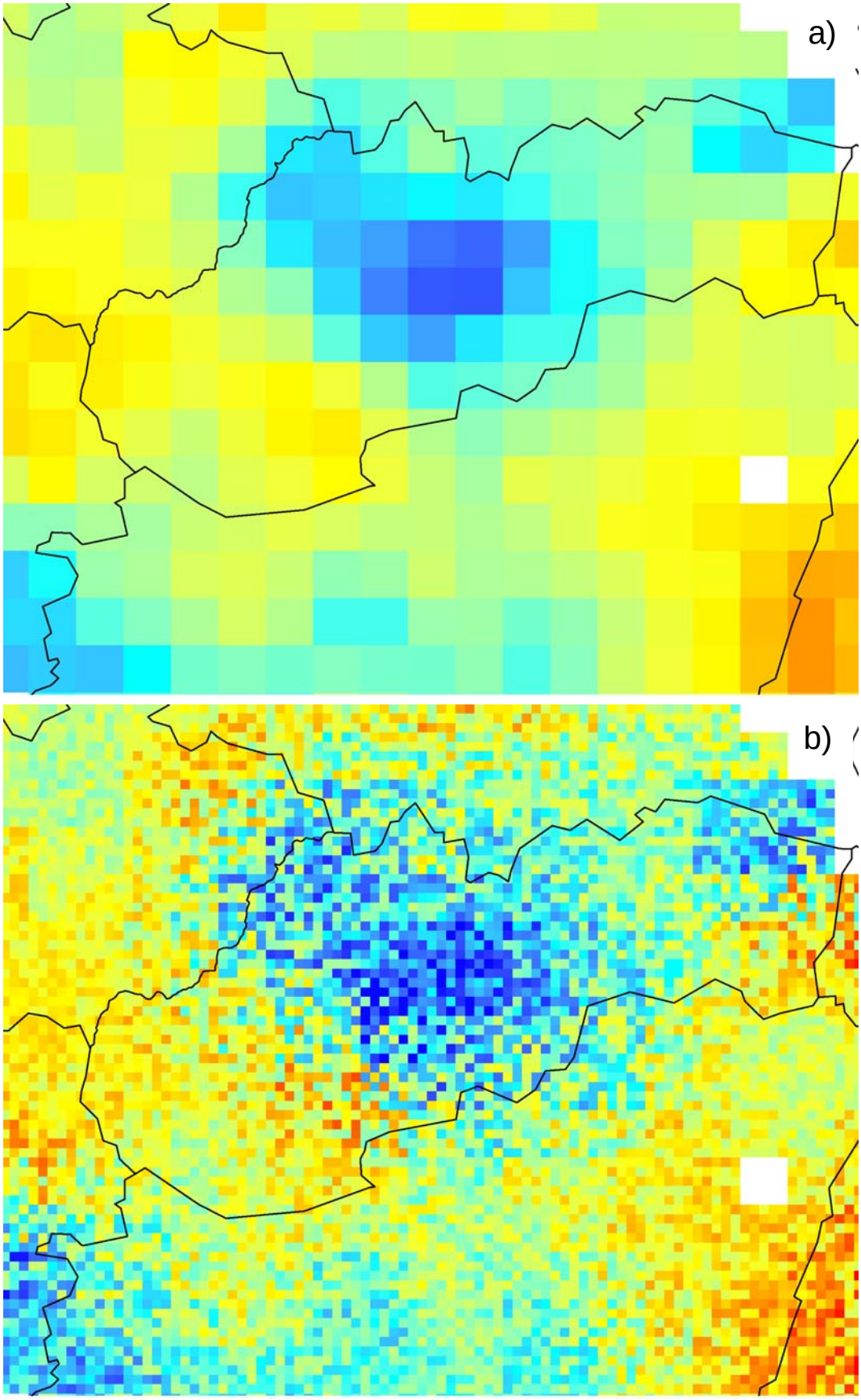

Figure 20: (a) Regional ERS scatterometer soil moisture, (b) Random downscaling – 2006-07-12 – detail Slovakia, Hungary

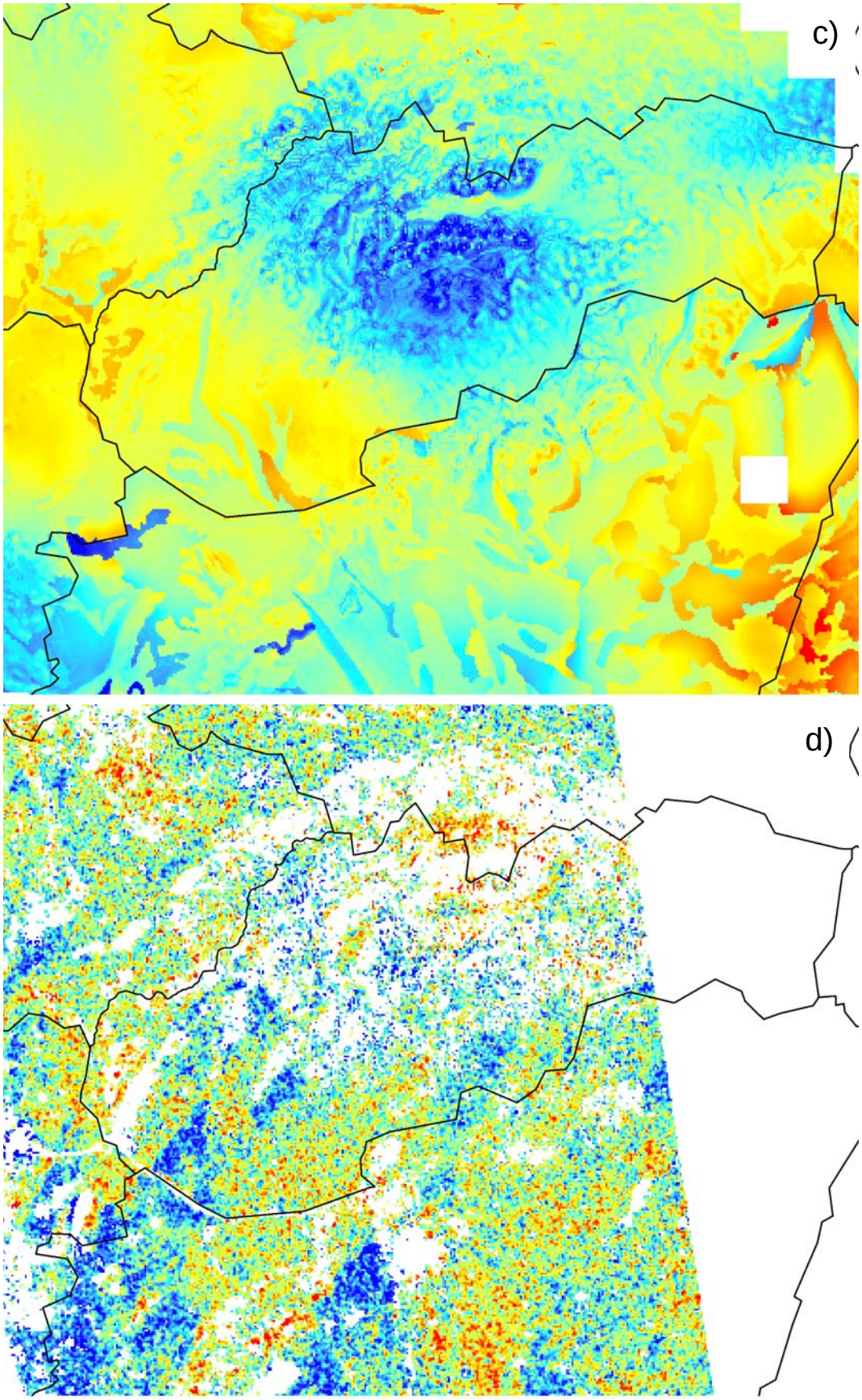

Figure 20: (c) Hydrological downscaling of ERS scatterometer soil moisture, (d) ENVISAT soil moisture – 2006-07-12 – detail Slovakia, Hungary

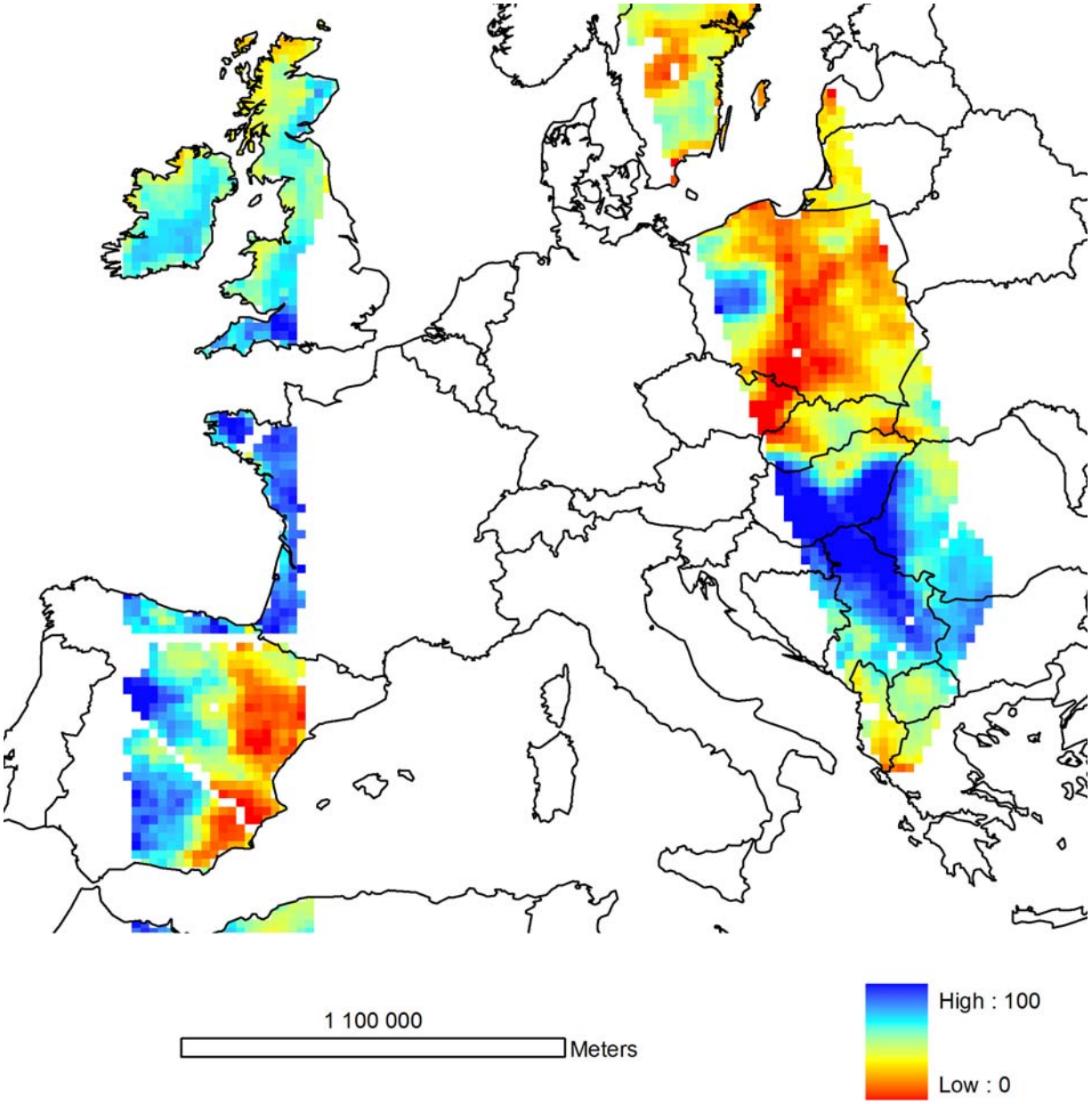

Figure 21a: Regional ERS scatterometer soil moisture – 2006-02-19

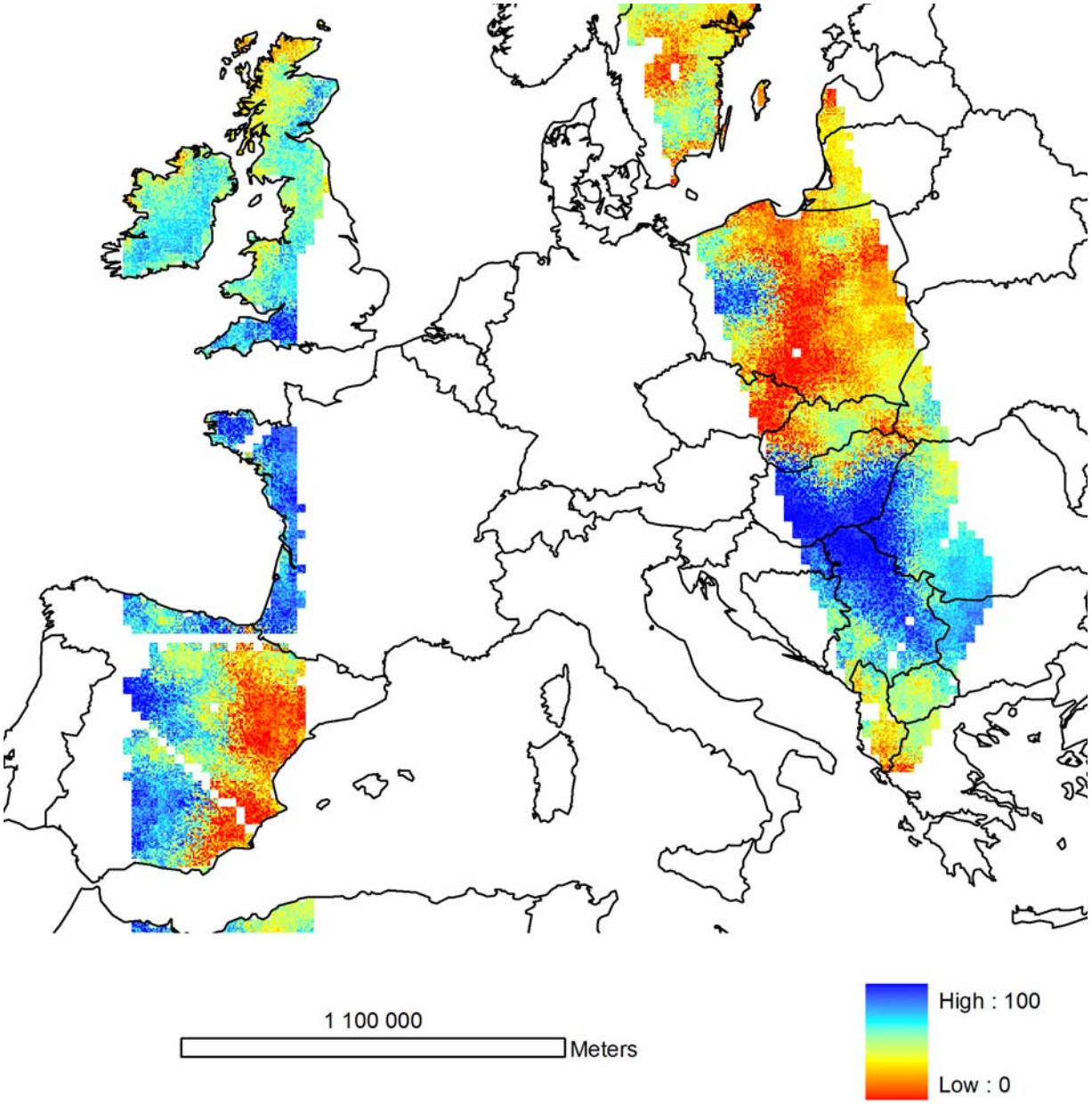

Figure 21b: Random downscaling - ERS scatterometer soil moisture – 2006-02-19

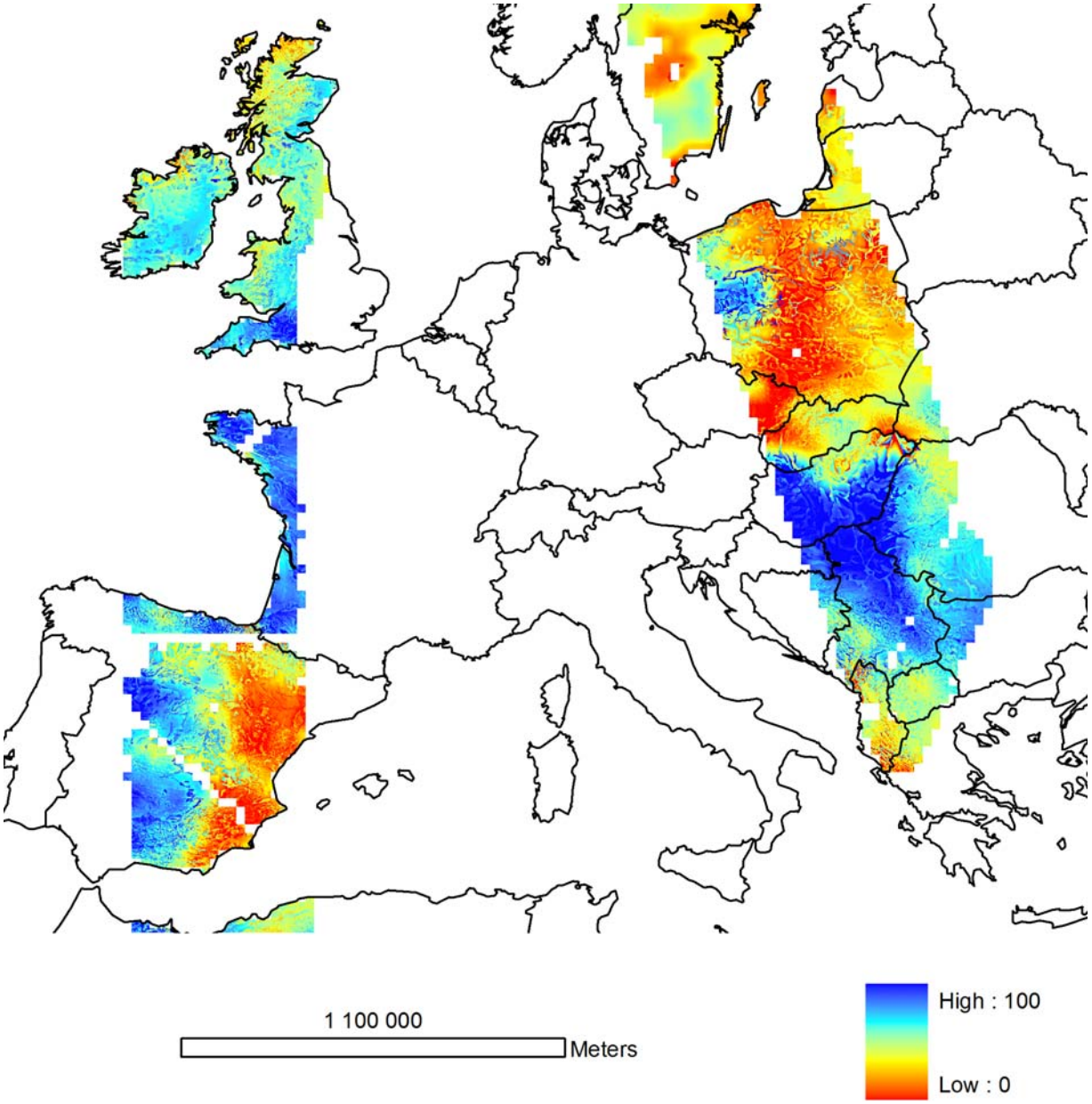

Figure 21c: Hydrological downscaling - ERS scatterometer soil moisture – 2006-02-19

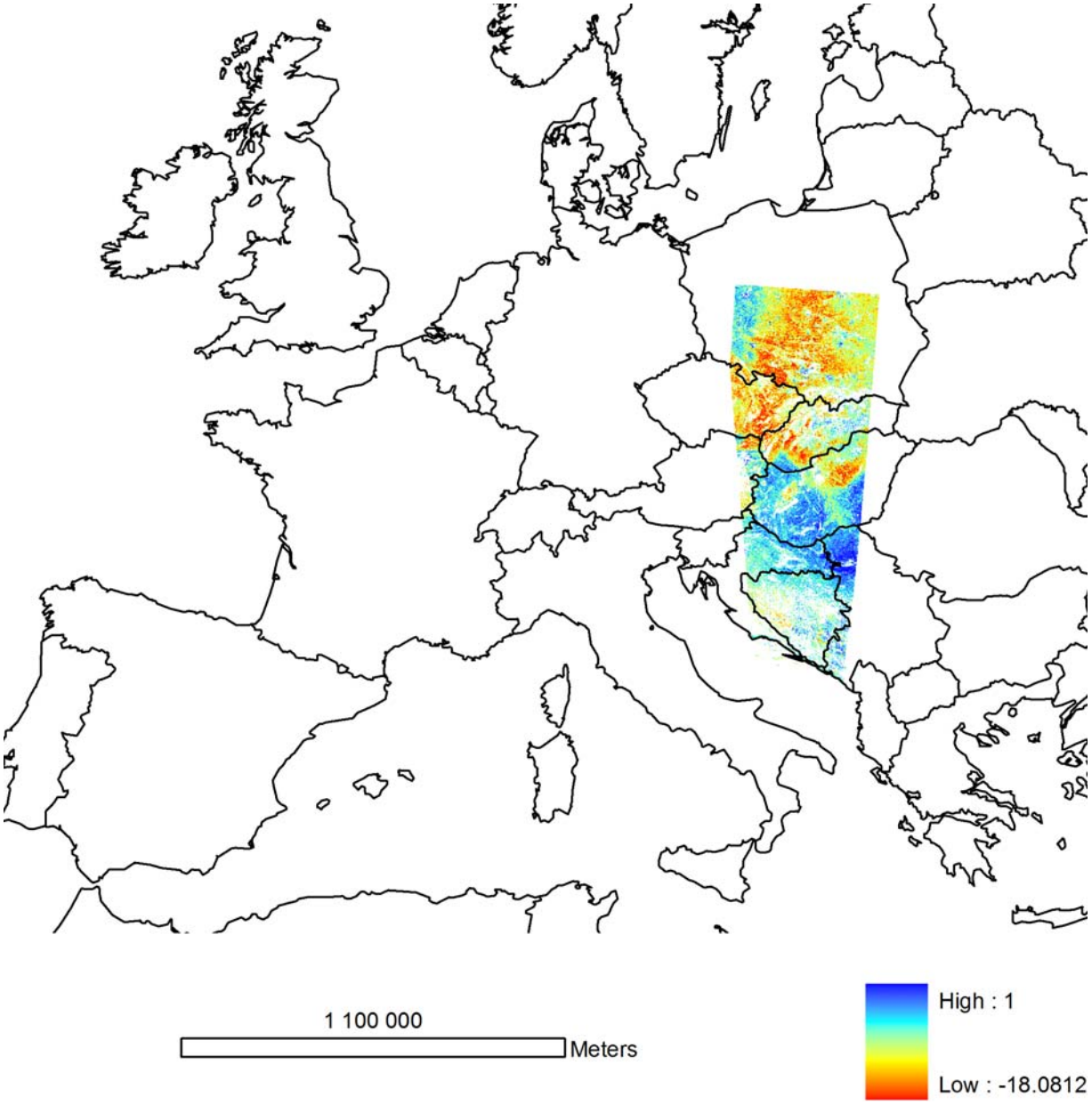

Figure 21d: Local ENVISAT soil moisture – 2006-02-19

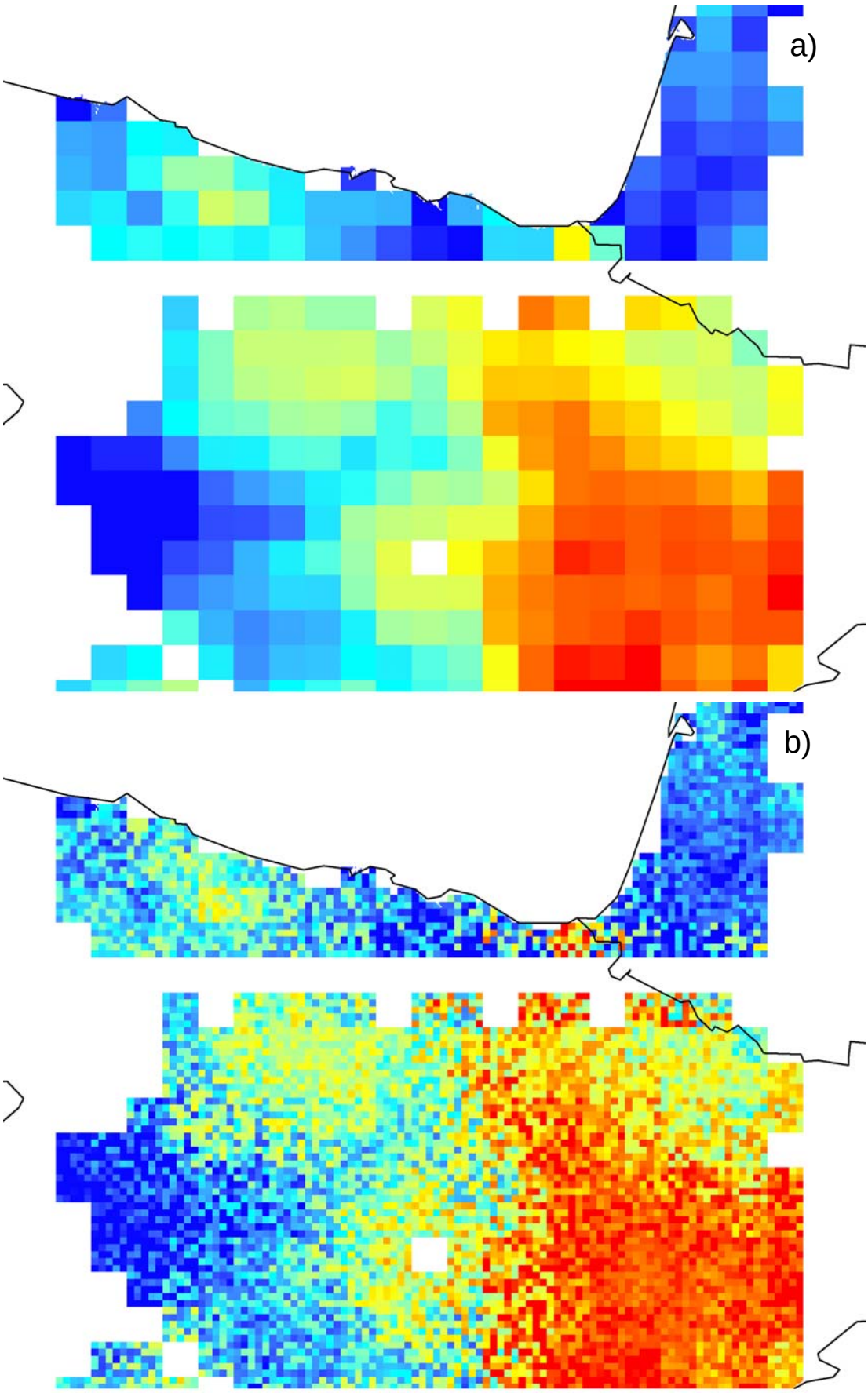

Figure 22: (a) Regional ERS scatterometer soil moisture, (b) Random downscaling – 2006-02-19 – detail Northern Spain

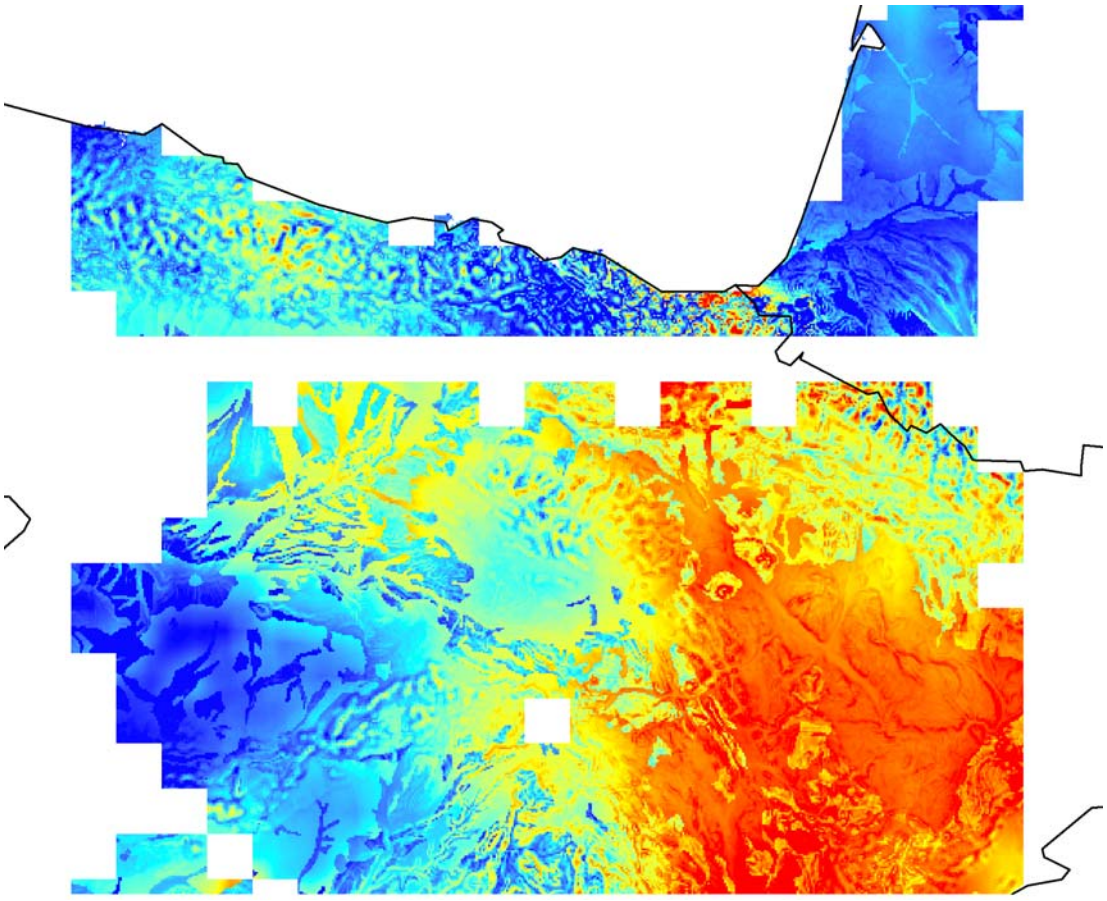

Figure 22: (c) Hydrological downscaling of ERS scatterometer soil moisture – 2006-02-19 – detail Northern Spain

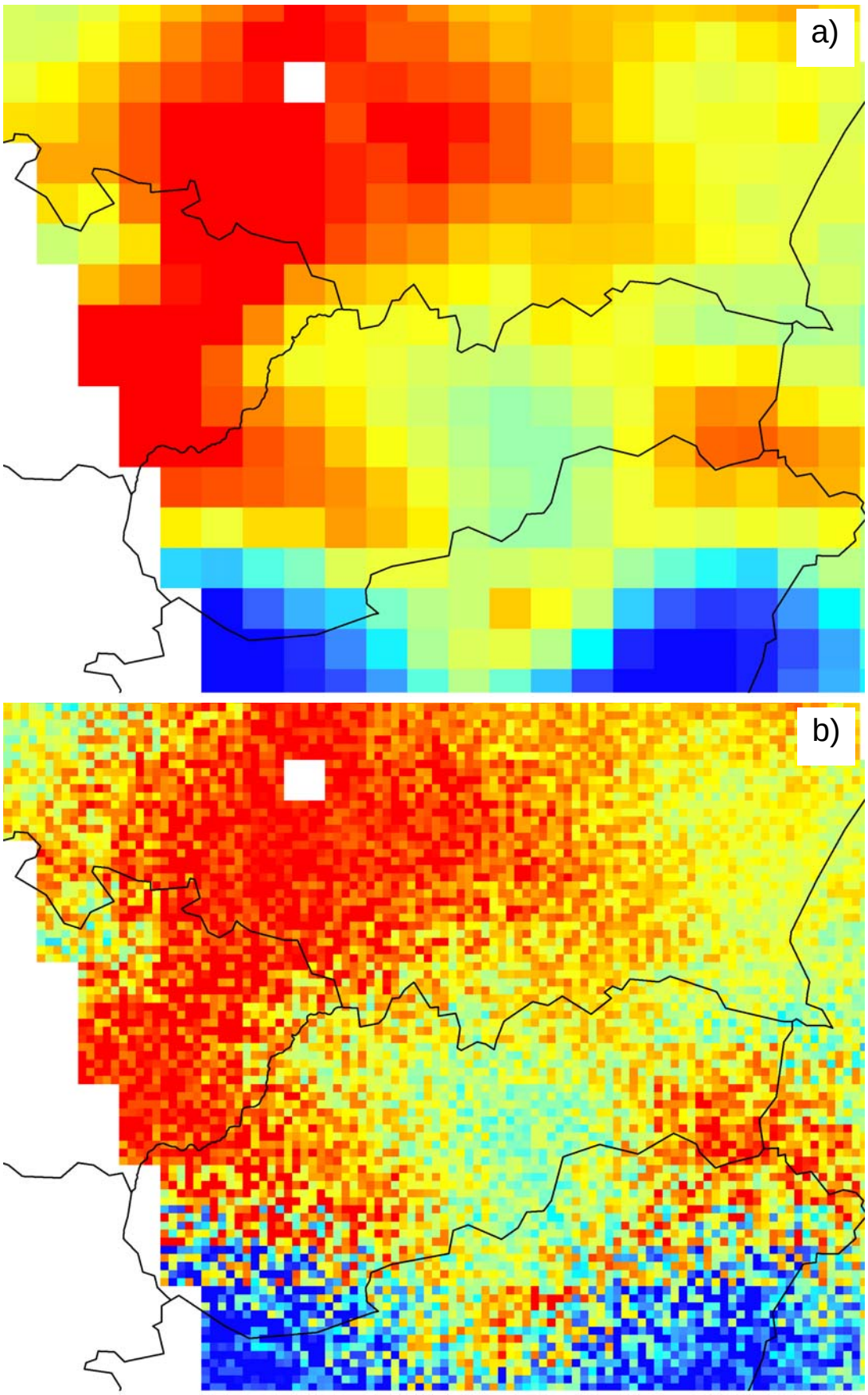

Figure 23: (a) Regional ERS scatterometer soil moisture, (b) Random downscaling – 2006-02-19 – detail Slovakia, Poland

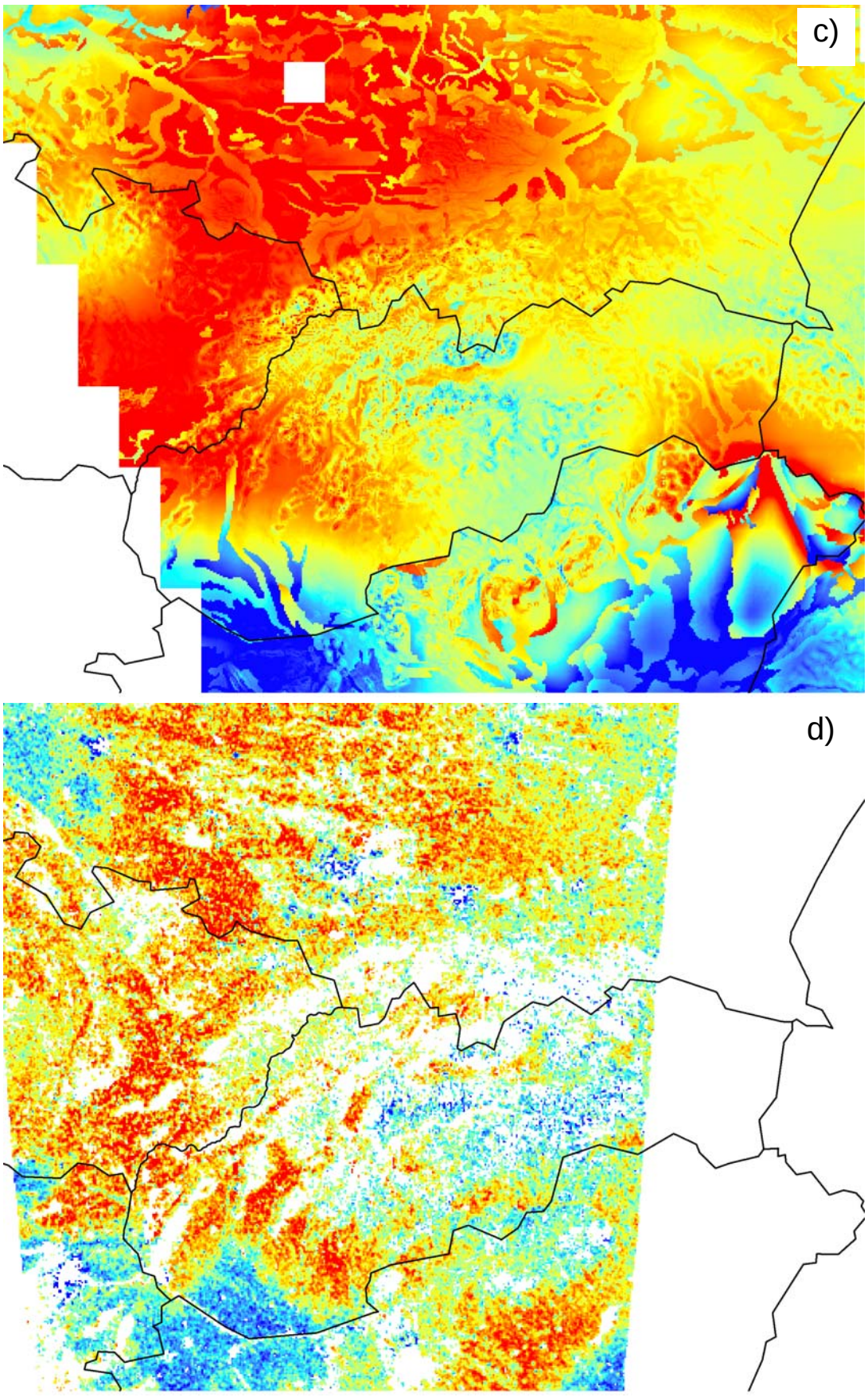

Figure 23: (c) Hydrological downscaling of ERS scatterometer soil moisture, (d) ENVISAT soil moisture – 2006-02-19 – detail Slovakia, Poland

4.5 Correlations with ENVISAT ASAR data

For a more quantitative assessment, the downscaled soil moisture patterns from the ERS Scatterometer were correlated with the ENVISAT data for each day individually. A correlation coefficient close to unity implies that the spatial patterns of the downscaled soil moisture and the ENVISAT data are similar. However, the correlations do not give information on the absolute values or the overall spatial variance of the downscaled pattern. Since the ENVISAT data are rather noisy, the correlations were performed for the average soil moisture values over 5 x 5 km areas.

The results for those four days when the spatial overlap between ERS-Scatterometer soil moisture and ENVISAT data was largest are presented in Table 2. These are the dates also shown in Figures 14 - 23. For July 12, 2006, using the original (regional scale) scatterometer data gives a correlation coefficient of 0.241 with the ENVISAT data. Using the random downscaling method decreases the performance slightly to a correlation coefficient of 0.217. However, using the hydrological downscaling method increases the performance slightly to a correlation coefficient of 0.248. For the other dates in Table 2, the hydrological downscaling gives slightly lower correlations than the original scatterometer data. This would be expected as the lack of small scale variability tends to favour variance measures such as the correlation coefficient. However, the hydrological downscaling method is consistently better than the random downscaling which adds credence to the plausibility of the method.

The correlation coefficient for all the days examined are shown in Figure 24. Each point relates to one day. Figure 24a gives the comparison of the correlation coefficients between regional scatterometer soil moisture and ENVISAT data with the correlation coefficients between hydrologically downscaled scatterometer soil moisture and ENVISAT data. Overall, the correlations with the hydrological downscaling methods tend to be slightly lower than those for the original scatterometer soil moisture, but the differences are very small.

Figure 24b gives the comparison of the correlation coefficients between randomly downscaled scatterometer soil moisture and ENVISAT data with the correlation coefficients between hydrologically downscaled scatterometer soil moisture and ENVISAT data. On most days, the correlations of the hydrological downscaling are higher than those of the random downscaling, indicating that the downscaling method proposed here does have predictive performance.

Table 2: Correlation coefficients between various downscaling variants of ERS Scatterometer soil moisture and ENVISAT data. The dates correspond to those indicated by circles in Figure 24.

Date of acquisition	Number of overlapping grid cells	Correlation coefficient		
		Regional (no downscaling) – ENVISAT	Random downscaling – ENVISAT	Hydrological downscaling – ENVISAT
2006-07-12	367035	0.241	0.217	0.248
2006-02-19	213407	0.823	0.790	0.806
2006-12-31	169322	0.841	0.823	0.842
2006-08-22	137454	0.455	0.408	0.440

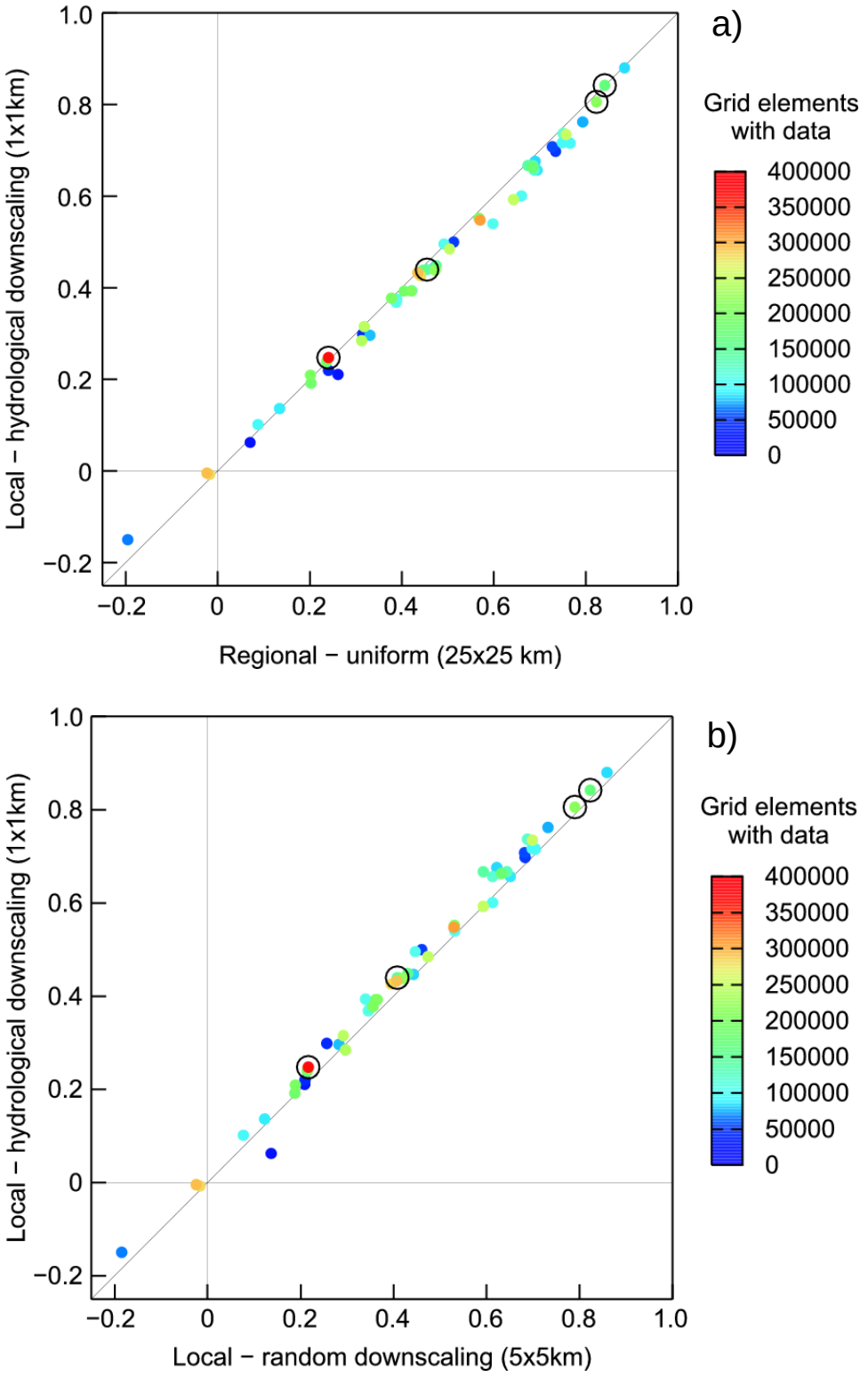

Figure 24: Performance of the downscaling methods: The vertical axes show the correlation coefficients between hydrologically downscaled ERS scatterometer soil moisture and ENVISAT data. The horizontal axes show (a) the correlation coefficients between regional ERS scatterometer soil moisture and ENVISAT data, and (b) the correlation coefficients between randomly downscaled ERS scatterometer soil moisture and ENVISAT data. Each point represents the spatial correlation on one day during 2005 to 2007. Colours indicate the number of grid elements with overlap and circles indicate the dates shown in Figures 13 - 23. Only days with significant overlap are shown.

5. Conclusions

There are two main outcomes from this project. The first is a new method that allows the downscaling of ERS scatterometer data to a spatial scale of 1 km that is more useful for hydrological applications. The method is based on hydrological indices and uses a minimum amount of data, so should be applicable to operational purposes.

The second outcome is information on how accurate the hydrological downscaling method is, as compared to using the original scatterometer data and to using a random downscaling method. The hydrological downscaling method gives indeed plausible patterns. They are better correlated to ENVISAT data than are the random downscaling results, but the correlations are slightly lower than those of the original scatterometer data. The latter result, however, does not imply that the original scatterometer data would be more suitable for hydrological applications as they lack small scale detail which is essential for hydrological applications.

The results demonstrate the feasibility of the method which will likely increase the potential of existing soil moisture scatterometer retrieval procedures developed as part of the H-SAF project, in particular for hydrological applications. However, it is suggested that more work is needed on examining the robustness of the method and on identifying optimum parameters of the conceptual hydrological model (Table 1). As the fingerprints are stationary they could also be used for downscaling average soil moisture values, e.g., soil moisture averaged over a number of years. Alternatively, the fingerprints can be straightforwardly extended to represent antecedent rainfall during the day before the soil moisture data were collected which would lead to a dynamic downscaling method.

6. References

Barling, R.D., Moore, I.D. and Grayson, R.B. (1994) A quasi-dynamic wetness index for characterizing the spatial distribution of zones of surface saturation and soil water content. *Water Resources Research*, 30(4), 1029-1044.

Beven K. (1995) Linking Parameters Across Scales: Subgrid Parameterizations and Scale Dependent Hydrological Models. *Hydrological Processes* 9, 507-525.

Beven, K. J. and Kirkby, M. J. (1979) A physically-based, variable contributing area model of basin hydrology. *Hydrol. Sci. Bull.*, 24, 43-69.

Blöschl, G. (1999) Scaling issues in snow hydrology. *Hydrological Processes*, 13, pp. 2149-2175.

Blöschl, G. (2001) Scaling in hydrology. *Hydrological Processes*, 15, pp. 709-711.

Blöschl, G. (2005) Statistical upscaling and downscaling in hydrology. Article 9 in: Encyclopedia of Hydrological Sciences, M. G. Anderson (Managing Editor), J. Wiley & Sons, Chichester, pp. 135-154.

Blöschl, G. and R. Grayson (2000) Spatial observations and interpolation. Chapter 2 in R. Grayson and G. Blöschl (Eds.) Spatial Patterns in Catchment Hydrology: Observations and Modelling. Cambridge University Press, Cambridge, pp. 17-50.

Deutsch, C.V. and Journel, A.G. (1992) GSLIB Geostatistical software library and user's guide. Oxford University Press, New York, 340 pp.

Entin, J.K., Robock, A., Vinnikov, K.Y., Hollinger, S.E., Liu,S., Namkhai, A. (2000) Temporal and spatial scales of observed soil moisture variations in the extratropics. *Journal of Geophysical Research*, 105(D9), 11865-11877.

Grayson R.B. and Western A.W. (1998) Towards areal estimation of soil water content from point measurements: time and space stability of mean response. *Journal of Hydrology* 207, 68-82.

Grayson, R. and Blöschl, G. (2000b) Summary of pattern comparison and concluding remarks. Chapter 14 in R. Grayson and G. Blöschl (Eds.) Spatial Patterns in Catchment Hydrology: Observations and Modelling. Cambridge University Press, Cambridge, UK, pp. 355-367.

Grayson, R. B. and G. Blöschl (Eds) (2000a) Spatial Patterns in Catchment Hydrology: Observations and Modelling. Cambridge University Press, Cambridge, UK, 404 pp.

Grayson, R., G. Blöschl, A. Western and T. McMahon (2002) Advances in the use of observed spatial patterns of catchment hydrological response. *Advances in Water Resources* 25, pp. 1313-1334.

Green, T.R. and R. H. Erskine (2004) Measurement, scaling, and topographic analyses of spatial crop yield and soil water content. *Hydrological Processes*, 18 (8) p 1447-1465.

Hu Z, Islam S, Cheng Y. (1997) Statistical characteriszation of remotely sensed soil moisture images. *Remote Sensing of the Environment* 61, 310-318.

Merz, R., Blöschl, G., Kirnbauer, R. (2001) Scale issues in regionalising flood frequencies. Proc. International Workshop on Scaling Problems in Hydrology, 7-8th June 2001, Vienna. Gutknecht et al. (eds.) Austrian Academy of Sciences, Vienna, pp. 155-174.

Mohanty, B.P., Skaggs, T.H. and Famiglietti, J.S. (2000) Analysis and mapping of field-scale soil moisture variability using high-resolution, ground-based data during the Southern Great Plains 1997 (SGP97) Hydrology Experiment. *Water Resources Research*, 36(4), 1023-1031.

Montaldo, N., and J.D. Albertson (2003) Temporal Dynamics of Soil Moisture Variability: 2. Implication for Land Surface Models, *Water Resources Research*, 39 (10), Art. No. 1275.

Moore, I.D., Grayson, R.B. and Ladson, A.R. (1991) Digital terrain modelling: A review of hydrological, geomorphological, and biological applications. Hydrological Processes, 5, 3-30.

Nyberg, L., (1996) Spatial variability of soil water content in the covered catchment at Gårdsjön, Sweden. *Hydrological Processes*, 10, 89-103.

O'Loughlin, E.M. (1986) Prediction of surface saturation zones in natural catchments by topographic analysis. *Water Resources Research*, 22(5), 794-804.

Pitman A.J. (2003) The evolution of, and revolution in, land surface schemes designed for climate models. *Int J Climatol* 23, 479-510, doi: 10.1002/joc.893

Ronda R. J., B. J. J. M. van den Hurk, A. A. M. Holtslag (2002) Spatial Heterogeneity of the Soil Moisture Content and Its Impact on Surface Flux Densities and Near-Surface Meteorology. *Journal of Hydrometeorology*, Vol. 3, No. 5, pp. 556–570.

Scipal, K (2002) Global Soil Moisture Retrieval from ERS scatterometer Data, PhD Thesis, Vienna University of Technology

Seyfried, M. (1998) Spatial variability constraints to modeling soil water at different scales. *Geoderma*, 85(2-3), 231-254.

Skøien, J. O., G. Blöschl and A. W. Western (2003) Characteristic space scales and timescales in hydrology. *Water Resources Research*, 39, (10), article number 1304.

Skøien, J.O. and G. Blöschl (2006a) Sampling scale effects in random fields and implications for environmental monitoring. *Environmental Monitoring and Assessment*, 114 (1-3), pp-521-552.

Skøien, J.O. and G. Blöschl (2006b) Scale effects in estimating the variogram and implications for soil hydrology. *Vadose Zone Journal*, 5, pp. 153-167.

Steinacker, R., M. Ratheiser, B. Bica, B. Chimani, M. Dorninger, W. Gepp, C. Lotteraner, S. Schneider and S. Tschannett (2006) A mesoscale data analysis and downscaling method over complex terrain. *Monthly Weather Review*, 134, 2758-2771.

Viney, N.R and M. Sivapalan (2004) A framework for scaling of hydrologic conceptualizations based on a disaggregation-aggregation approach. *Hydrological Processes*, 18 (8) p 1395-1408.

Wagner, W., G. Lemoine,.H. Rott (1999): A Method for Estimating Soil Moisture from ERS Scatterometer and Soil Data. Rem. Sens. Environ. 70: 191-207.

Wagner, W. K. Scipal, C. Pathe, D. Gerten, W. Lucht, B. Rudolf (2003) Evaluation of the agreement between the first global remotely sensed soil moisture data with model and precipitation data, *Journal of Geophysical Research – Atmospheres*, Vol. 108, No. D19, 4611, doi: 10.1029/2003JD003663.

Wagner, W., C. Pathe, M. Doubkova, D. Sabel, A. Bartsch, S. Hasenauer, G. Blöschl, K. Scipal, J. Martínez-Fernández and A. Löw (2008) Temporal stability of soil moisture and radar backscatter observed by the Advanced Synthetic Aperture Radar (ASAR). *Sensors*, 8 (2), pp. 1174-1197.

Western, A. W. and G. Blöschl (1999) On the spatial scaling of soil moisture. *Journal of Hydrology*, 217, pp. 203-224.

Western, A. W., G. Blöschl and R. B. Grayson (1998) Geostatistical characterisation of soil moisture patterns in the Tarrawarra catchment. *Journal of Hydrology*, 205, pp. 20-37.

Western, A. W., R. B. Grayson, G. Blöschl, G. R. Willgoose and T. A. McMahon (1999) Observed spatial organisation of soil moisture and its relation to terrain indices. *Water Resources Research*, 35(3), pp. 797-810.

Western, A. W., S.-L. Zhou, R. B. Grayson, T. A. McMahon, G. Blöschl and D. J. Wilson (2004) Spatial correlation of soil moisture in small catchments and its relationship to dominant spatial hydrological processes. *Journal of Hydrology*, 286 (1-4), pp. 113-134.

Western, A., R. Grayson and G. Blöschl (2002) Scaling of soil moisture: a hydrologic perspective, *Ann. Rev. Earth and Planetary Sci.*, 30, pp. 149–180.

Western, A.W., R.B. Grayson, G. Blöschl and D. J. Wilson (2003) Spatial variability of soil moisture and its implications for scaling. In: Y. Pachepsky, D.E. Radcliffe, H.M. Selim and (Eds.), Scaling methods in soil physics. CRC Press, Boca Raton, pp. 119-142.

Wilson, J.P. and Gallant, J.C. (Editors) (2000) Terrain analysis: principles and applications. John Wiley, New York.

Wood, E.F., Lettenmaier, D.P. and Zartarian, V.G. (1992) A land-surface hydrology parameterization with subgrid variability for general circulation models. *Journal of Geophysical Research*, 97(D3), 2717-2728.

Woods RA, Sivapalan M, Robinson JS. (1997) Modeling the spatial variability of subsurface runoff using a topographic index. *Water Resources Research* 33, 1061-1073.

Zehe, E., and G. Blöschl (2004), Predictability of hydrologic response at the plot and catchment scales: Role of initial conditions, *Water Resources Research*, 40 , W10202, doi:10.1029/2003WR002869.

Zhao, R.-J. (1992) The Xinanjiang model applied in China. *Journal of Hydrology*, 135, 371-381.